ACTA
FORESTALIA
FENNICA
187

MEASUREMENT OF FLUCTUATING IRRADIANCE IN FIELD STUDIES OF PHOTOSYNTHESIS

SÄTEILYN VAIHTELUN MITTAAMINEN FOTOSYNTEESIN MAASTOTUTKIMUKSISSA

Heikki Smolander

SOCIETAS FORESTALIS FENNIAE

SUOMEN METSÄTIETEELLINEN SEURA 1984

Suomen Metsätieteellisen Seuran julkaisusarjat

ACTA FORESTALIA FENNICA. Sisältää etupäässä Suomen metsätaloutta ja sen perusteita käsitteleviä tieteellisiä tutkimuksia. Ilmestyy epäsäännöllisin väliajoin niteinä, joista kukin käsittää yhden tutkimuksen.

SILVA FENNICA. Sisältää etupäässä Suomen metsätaloutta ja sen perusteita käsitteleviä kirjoitelmia ja lyhyehköjä tutkimuksia. Ilmestyy neljästi vuodessa.

Tilaukset ja julkaisuja koskevat tiedustelut osoitetaan seuran toimistoon, Unioninkatu 40 B, 00170 Helsinki 17.

Publications of the Society of Forestry in Finland

ACTA FORESTALIA FENNICA. Contains scientific treatises mainly dealing with Finnish forestry and its foundations. The volumes, which appear at irregular intervals, contain one treatise each.

SILVA FENNICA. Contains essays and short investigations mainly on Finnish forestry and its foundations. Published four times annually.

Orders for back issues of the publications of the Society, and exchange inquiries can be addressed to the office: Unioninkatu 40 B, 00170 Helsinki 17, Finland. The subscriptions should be addressed to: Academic Bookstore, Keskuskatu 1, SF-00100 Helsinki 10, Finland.

ACTA FORESTALIA FENNICA 187

MEASUREMENT OF FLUCTUATING IRRADIANCE IN FIELD STUDIES OF PHOTOSYNTHESIS

Heikki Smolander

Seloste

SÄTEILYN VAIHTELUN MITTAAMINEN FOTOSYNTEESIN MAASTOTUTKIMUKSISSA

To be presented, with the permission of the Faculty of Forestry of the University of Joensuu, for public criticism in Auditorium M1 of the University, Yliopistokatu 7, Joensuu, on 22 March 1985 at 12 o'clock noon.

HELSINKI 1984

SMOLANDER, H. 1984. Measurement of fluctuating irradiance in field studies of photosynthesis. Seloste: Säteilyn vaihtelun mittaaminen fotosynteesin maastomittauksissa. Acta For. Fenn. 187: 1–56.

The problems caused by the temporal and spatial microvariation in irradiance during field measurements of photosynthesis are studied. It is concluded on the basis of variation analyses based on irradiance data measured in a Scots pine (*Pinus sylvestris* L.) stand that the microvariation should be measured by integrating it over the measurement time and space.

However, the curvilinearity of the light response of photosynthesis results in biased estimates when linear integration (mean irradiance) is used. The significance of the bias is examined using a simulation technique on irradiance material. Wether the actual integral of photosynthesis can be approximated with mathematical methods is next studied. The methods were second order Taylor series approximation and two-point distribution approximation. The former method gave satisfactory results only for a low curvature response, but the latter method was applicable also to the high curvature response. However, both methods presuppose that the mean and variance are known. Measurement of the variance is based on integration of the second power.

A new method, where the nonlinearity problem is avoided, is presented to measure fluctuation of the irradiance. The method enables the shoot geometry to be taken into account and it is also applicable to transpiration studies.

Tutkimuksessa tarkastellaan säteilyn ajallisen ja paikallisen mikrovaihtelun fotosynteesin maastomittauksissa aiheuttamia ongelmia. Männiköstä (*Pinus sylvestris* L.) kootusta säteilyaineistosta tehtyjen hajontatarkastelujen perusteella tullaan siihen johtopäätökseen, että mikrovaihtelu on mitattava integroimalla se mittaustapahtuman, so. ajan ja paikan yli.

Fotosynteesin valovasteen käyräviivaisuus aiheuttaa kuitenkin keskimääräistä irradianssia (lineaarista integrointia) käytettäessä harhaa tuloksiin. Harhan merkitystä tarkastellaan simulointitekniikalla männikössä mitatun valoaineiston perusteella. Tämän jälkeen tutkitaan, voiko matemaattisin menetelmin approksimoida todellista integraalia laskennallisesti. Tutkitut menetelmät olivat Taylorin sarjakehitelmä ja jakauman approksimointi. Edellinen antoi tyydyttäviä tuloksia vain loivalle valovasteelle, mutta jälkimmäinen soveltui myöskin jyrkän valovasteen tapaukseen. Molemmat menetelmät edellyttävät, että keskiarvon lisäksi tunnetaan myös varianssi. Varianssin mittaus on palautettavissa neliön integroinniksi.

Tulosten perusteella esitetään uusi valonmittausmenetelmä, jossa kuvattu epälineaarisuusongelma on vältetty, ja joka fysikaalisesti selkeänä mahdollistaa myöskin mittausgeometrian ottamisen mukaan laskentavaiheessa.

ODC 111.21--015+111.84
ISBN 951-651-064-7
Arvi A. Karisto Oy:n kirjapaino
Hämeenlinna 1984

CONTENTS

PREFACE

The problem treated in this study gradually became apparent while I was working as a member of the Primary Production Group at the Department of Silviculture, the University of Helsinki. The study formed part of a wider investigation of the ecophysiology of trees, which had been carried out at Hyytiälä since the beginning of the 1970's.

The discussions I had with Pekka Kauppi, Lic For, Raimo Salminen, Lic Tech, and Mr Timo Tamminen played a major role in the formulation of the study. Mr Tamminen also collected the data used in the study. I have received advice and help in calculations from Juha Lappi, M Sc, Pauline Oker-Blom, M Sc, and Erkki Siivola, M Sc.

In addition to the above-mentioned persons, Henrik Eckersten, M Sc, Prof Pekka Kilkki, Ahti Kotisaari, M Sc, Tapani Lahti, M Sc, Prof Paavo Pelkonen, Dr Veli Pohjonen, Docent Kurt Perttu and Pasi Puttonen, Lic For, have read and made comments during the various stages in the preparation of the manuscript. I am exceedingly grateful to them for their constructive criticism.

I would like to thank my supervisors, Prof Matti Leikola and Prof Seppo Kellomäki for their support, and the Head of the Suonenjoki Research Station, Dr. Pertti Harstela, and Head of the Department of Silviculture, Prof Erkki Lähde, both from the Finnish Forest Research Institute, for their accommodating attitude towards my work. I would also like to extend my grateful thanks to my colleaques in the Primary Production Group and to fellow researchers and staff at Suonenjoki Research Station. I wish express my sincere thanks to the Academy of Finland and to Niemi-Foundation for the financial support offered for this study.

Mrs Sinikka Jauhiainen and Ms Sari Nahkuri have, with extreme skill and patience, drawn the figures and graphs. The original manuscript was translated into english by John Derome, M Sc. To them, my warmest thanks for their assistance.

Finally, I would like to thank my wife Annmarie and sons Sampo and Tuomo for their understanding and support.

Suonenjoki, November 1984

Heikki Smolander

1. INTRODUCTION

Solar radiation (or short-wave radiation, 300–3000 nm) is the driving force for the transpiration and photosynthesis of all green plants. The visible radiation (400–700 nm) is utilized in photosynthesis. Radiation of longer wavelength is important for transpiration affecting the heat balance of leaves. The effect of solar radiation on photosynthesis and transpiration has been extensively studied for a long time (see e.g. Gates 1980). Another important research problem is the behaviour of radiation inside stands. This special branch of meteorology is called actinometry (e.g. Ross 1981). Actinometry has developed into a separate field of science which is more allied to crop science than to meteorology.

Radiation differs in many respects from the other environmental factors which have an effect on photosynthesis and transpiration. First of all, it varies temporally already above the stand and even more so within the stand. In addition to the temporal variation, there is also large spatial variation inside the stand. Another important feature is that the direction distribution of the radiation flux changes as a function of time. The other environmental factors, such as air temperature and humidity, are diffuse and they vary more slowly. Changes in the speed and direction distribution of the wind also exhibit features similar to those of light, but the importance of wind for photosynthesis is much less.

The method of measuring radiation is determined by the ultimate use of the data (e.g. Hari et al. 1982). If the aim is to determine the amount of carbon dioxide assimilated by a specific shoot during a period of one year, then relatively simple methods can be used for characterizing the prevailing radiation conditions. On the other hand, if the objective is to study the physiological mechanisms associated with photosynthesis, then the demands set on the measurement method are considerably greater. The radiation measurements must be valid for the photosynthesis measurements. If there are deficiencies in the validity of the radiation measurements, changes in the environment or structure of the measuring point can erroneously be interpreted as physiological changes.

The ecophysiological theories of gas exchange are primarily based on the mechanistic model of gas exchange presented by Gaastra (1959). This so-called diffusion model has been further developed by, among others, Chartier (1970), Charles-Edwards and Ludwig (1974), and Farquhar et al. (1980a). In this sort of approach it is essential to distinguish between the driving force and factors slowing down diffusion. The driving force of the gas diffusion is the partial pressure difference of the gas. The main factors slowing down the gas diffusion are cuticular, stomatal and boundary layer resistances. Utilization of the model presupposes that the rates of the processes are measured in a physically relevant way, since the driving forces and flow resistances are separated from each other by mathematical means. On the other hand, theoretical research on the connections between photosynthesis and transpiration has shown that these processes cannot be interpreted as separate entities without causing problems in the interpretation of the results (e.g. Farquhar et al. 1980b). For this reason, the environmental factors should be measured in such a way that the data is applicable to the analysis of both processes.

In order to calculate the driving force of CO_2 uptake, i.e. the difference between the ambient and intercellular CO_2 concentrations (C_a–C_i), the ambient CO_2 concentration and the magnitude of the leaf resistance (boundary layer and stomatal resistance) must be known. The stomatal resistance can be calculated on the basis of transpiration, ambient H_2O concentration and the leaf temperature. In this case it is assumed that the intercellular air space is saturated with water vapour. The inputs of the mechanistic gas exchange model are thus: CO_2 and H_2O fluxes, the ambient CO_2 and H_2O concentrations, and leaf temperature. Thus the driving forces and diffusion resistances are quantities which are calculated from the above quantities using the physical laws of gas diffusion.

Among the quantities to be measured, leaf temperature has proved to be the most difficult from the point of view of continuous measurements (e.g. Christersson and Sandstedt 1968, Lange 1962, Linder et al. 1980). It can also be measured indirectly if a reliable estimate of the amount of radiation absorbed by the leaf can be obtained (e.g. Raschke 1956). Under natural conditions, the wind also has an effect on the heat balance, but its effect is stabilized in photosynthetic measurements as a result of the measuring technique used. The percentage of photosynthetically active radiation (PAR) out of the global radiation is fairly constant, 50 % for a free horizon, (Szeicz 1974). Thus the flux density of short wave radiation can be derived approximately from the flux density of PAR. As the amount of PAR is the most important environmental factor for the interpretation of photosynthetic measurements, considerable attention must be paid to the validity of its measurement.

The unexplained variation in the light responses of photosynthesis measured in the field is greater than that encountered in laboratory experiments. Although this difference is quite considerable and regular, the biological and methodological causes of this phenomenon have been largely neglected in the literature. The most obvious biological cause is the hysteresis associated with the water balance (e.g. Troeng and Linder 1978). The methodological causes are primarily associated with the properties of the radiation field and the methods used to characterize it. First and foremost, the radiation field in laboratory measurements is temporally and spatially stable. In field measurements of photosynthesis, large temporal and spatial variation is encountered. In addition, the direction distribution of the radiation flux is also stable in laboratory set-ups. If the radiation flux density is regulated by varying the distance to the radiation source, the direction distribution of the radiation varies only slightly. In field measurements, however, the passage of the sun across the sky produces changes in the direction distribution of the radiation field with respect to time.

The aim of this study is to determine physically unambiguous means of measuring radiation in field studies of photosynthesis and traspiration in accordance with the gas exchange model presented by Gaastra (1959). The study is mainly concerned with problems caused by temporal and spatial variation in radiation which makes the analysis and interpretation of field measurements difficult. The problems associated with the direction distribution of the radiation field are outside the scope of this study, but are discussed here when encountered in the measurement of the temporal and spatial variation of the radiation flux density.

2. THE RESEARCH PROBLEM

21. Measurement of irradiance fluctuation in field studies of photosynthesis

The curvilinearity of the light response of photosynthesis has been considered to cause many problems in photosynthesis models covering the whole stand (e.g. Ross 1970, Kellomäki et al. 1979) because it makes the use of average values difficult. Similarly, it causes problems in field measurements of photosynthesis. Methods of gas exchange monitoring can only measure the photosynthesis occurring during longer periods of time, eg. 10–200 seconds. During that period of time the light conditions can vary considerably (e.g. Anderson 1971). Local microvariation causes similar problems because the measurements usually have to be carried out on whole shoots – as is often intentionally done – or even small branches.

The methodological problems caused by microvariation can, in principle, be reduced by shortening the measurement period and reducing the size of the object being measured, i.e. by approaching point measurement or ideal measurements (Hari et al. 1983). For instance, use of equipment which could measure the photosynthesis of a single needle during one second could considerably reduce the problems associated with microvariation. Development of such equipment is presumably technically very difficult. Since only a few attempts have been made along these lines (cf. Jarvis et al. 1971), most studies remain at the plant level and utilise longer measurement periods (e.g. Hari et al. 1979, Linder et al. 1980, Kaufman 1981). The latest CO_2 porometers fulfil rather well the demands set by the principle of point measurements with respect to space in measurements on broadleaves (e.g. Schulze et al. 1982).

An approach which has proved to be superior to any basic development of gas exchange measurement techniques, involves taking the microvariation into account in the light measuring system itself. Various solutions have been developed in a number of different studies.

The problems associated with microvariation were avoided in the SWECON project by carrying out measurements in a lightly stocked stand where the local microvariation was small, and measuring the temporal microvariation by means of integration (1 minute, Linder et al. 1980). However, the error caused by the curvilinearity of the light response of photosynthesis was not eliminated.

A rather radical new approach which eliminates the problems associated with microvariation was developed by the Finnish Primary Production Group (University of Helsinki, Department of Silviculture). The developed measuring system takes into account both the temporal and spatial microvariation, and also the curvilinearity of the light response of photosynthesis (Hari et al. 1976). The measuring system "simulates" photosynthesis by integrating the light response of photosynthetic rate over time and space. The light response of the plant or shoot being measured is thus already built into the measuring device itself. This presupposes that the light response is known in advance accurately and that it does not vary excessively during the experiment. The measuring system has been used for measuring photosynthesis within the canopy (Hari et al. 1976, Pelkonen 1980), and also in measurements carried out in the open (Hallman et al. 1978, Pelkonen 1980).

Although the method has been successful in studying short-term variations of photosynthesis (Hari et al. 1981), it has proved to be problematic in the analysis of situations where the shape of the light response has probably varied (e.g. Pelkonen 1981, Smolander, unpublished data). This is due to the fact that the application of the method presupposes that the light response is known precisely up to the multiplicative constant (see Fig. 2.1). Many of the factors which have an effect on photosynthesis, especially environmental stress factors such as water stress, alter the shape of the light response curve (e.g. Marshall and Biscoe 1980ab). The effect of temperature on photosynthesis also follows the principle of limiting factors, and hence cannot be modelled using multiplicative models (e.g. Charles-Edwards 1981).

It appears from the above that the temporal and spatial microvariation have to be measured in field measurements of photosynthesis by means of integration, and that the features associated with nonlinear integration may cause problems in the analysis. It is thus worth studying the different possibilities of estimating the integrals of the photosynthetic light response functions with respect to time and space.

22. The non-linearity problem

In order to understand the problem of non-linearity, it is first necessary to define the amount of radiation available for photosynthesis which falls on a unit area during a unit of time. Let us first assume that the time constants of the light sensor and photosynthesis are of the same order of magnitude. The rate of photosynthesis, P, then follows the variation in the irradiance, I, by the response:

$$P = P(I) \qquad (2.1)$$

Irradiance varies on the horizontal plane with respect to both time, t, and space, X:

$$P = P(I(t,X)) \qquad (2.2)$$

Thus the mean photosynthesis of a unit area A, which can for instance be interpreted as the effective area of a leaf, during a specific period of time (t_0,t_1), is obtained by integrating:

$$\bar{P}(t_0, t_1; A) = \frac{1}{(t_1-t_0)A}\int\int_{t_0 A}^{t_1} P(I(t,A))\,dA\,dt \qquad (2.3)$$

The mean photosynthesis ($\bar{P}$) defined in Eq. (2.3) is the quantity to which the results obtained by simulating different measuring principles will be compared. It should be pointed out that integration over time and space is equivalent to integration over the irradiance distribution, if the rate of photosynthesis is dependent only on irradiance.

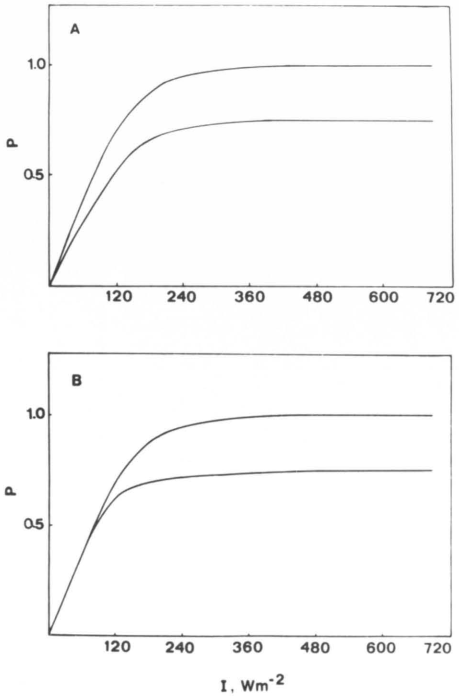

Fig. 2.1. The use of nonlinear integration presupposes that only the multiplicative constant of the light response varies (A). The effect of many environmental factors on the photosynthetic light response follows the principle of limiting factors (B).

The different principles involved in non-linear and linear integration are illustrated in Fig. 2.2. In the former case the transformation from irradiance to "photosynthesis" is carried out first, followed by integration over time and space. In the latter case the integration is accomplished first and the transformation then done from the mean irradiance $\bar{I}$. The latter technique always results in an incorrect estimate for photosynthesis if the light conditions vary. Carrying out the transformation in the calculation phase would, however, be practical because it would not be necessary to use a certain light response in the measurement stage.

The estimate for mean photosynthesis based on linear integration, $\hat{P}_L$ is:

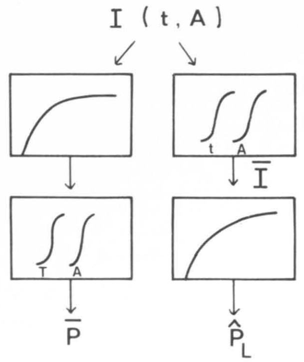

Fig. 2.2. Principle of linear (on the right) and nonlinear (on the left) integration.

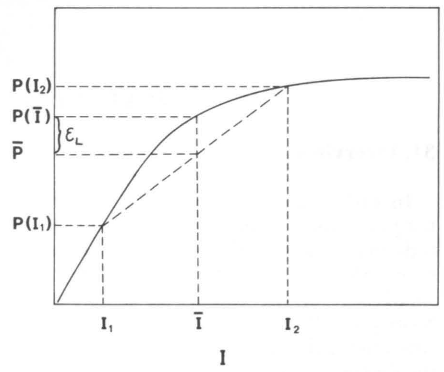

Fig. 2.3. Formation of the error due to linear approximation in the case of two observations.

$$\hat{P}_L = \hat{P}_L(t_0, t_1; A) = P(\bar{I});$$
$$\bar{I} = \frac{1}{(t_1-t_0)A}\int\int_{t_0 A}^{t_1} I(t,A)\,dA\,dt \qquad (2.4)$$

And further the error due to linear approximation, ε_L, is defined as:

$$\varepsilon_L = \hat{P}_L - \bar{P} \qquad (2.5)$$

As the light response of photosynthesis is concave it can be stated that

$$\varepsilon_L \geq 0. \qquad (2.6)$$

Formation of the error in the case of two points (observations) is illustrated in Fig. 2.3. It can be seen from the figure that the error is big when the response is most curved and correspondingly small when the response is nearly linear. It is also evident from the figure that the error increases as the variation in the irradiance becomes greater. The magnitude of the error is thus dependent on the relationship between the shape of the light response and the irradiance distribution within the period.

The expectation of the error, ε_L, is thus not zero, i.e. $\hat{P}_L$ is not an unbiased estimate of P. This is a feature which becomes methodologically more difficult, the longer is the integration period. This is because the bias results in accumulation of the error with the integration. If the irradiance behaves stationarily, then the error approaches a particular percentage limit value as the length of the integration period increases.

23. The study procedure

The first parts of this study (Sections 4 and 5) are concerned with the small-scale variation in the canopy of a Scots pine (*Pinus sylvestris* L.) stand with respect to time and space at a horizontal plane. Both the temporal and spatial microvariation are quantified by analysing standard deviation and skewness. In addition, the variation is described by means of autocorrelation functions. The significance of the variation is then estimated from the point of view of photosynthesis measurement by examining the integration problem caused by linear integration. A number of different computational methods for producing the integrals of irradiance available for photosynthesis are then examined. Methods for solving integration problems are presented on the basis of the results. Finally, the applicability of the presented method in solving other problems associated with radiation and photosynthesis measurement is evaluated.

3. MATERIALS AND METHODS

31. Overview

In order to get an overall picture of the temporal and spatial variation in the irradiance during photosynthesis measurement, the variation in the irradiance in a small part of the canopy of a 20-year-old Scots pine (*Pinus sylvestris* L.) stand was measured using the smallest available sensor over the shortest possible time interval. The aim of the experiment was to obtain data of the variation under different weather types and sun positions.

The measuring equipment used for determining this time-space variation consisted of a horizontal array of light sensors placed in a canopy, a light sensor in the open, and a data acquisition system. Data was collected with a programmable datalogger and the data was fed into a minicomputer (Fig. 3.1). Owing to the intensivity of the measurements, quite short measuring periods and a short array of sensors were used in this experiment.

A more representative material, consisting of frequency distributions of the irradiance collected with respect to time in different parts of the canopy, was used to study the temporal variation in more detail. The material was collected using the Eos system (Salminen et al. 1983), which consists of 32 light sensors located in different parts of the crown, and a programmed datalogger which collects and stores the observations in a distribution form. The principle of the Eos system is illustrated in Fig. 3.2.

32. Measuring equipment

321. The light sensor

The light sensors used in the experiment were constructed at the Applied Electronics Laboratory of the Helsinki University of Technology (Salminen et al. 1983). The structure and dimensions of the sensor are presented in Fig. 3.3 and its spectral properties in Fig. 3.4. The sensors have been calibrated using a Lambda pyranometer so that the output voltage is 0.1 mV/(Wm^{-2}), with a 1 % tolerance. The sensor obeys the cosine law well (Fig. 3.5).

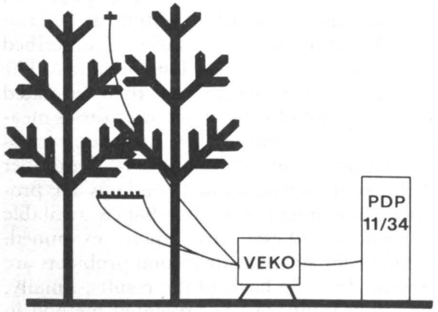

Fig. 3.1. Schematic representation of the measurement system used in measuring time-space variation of irradiance.

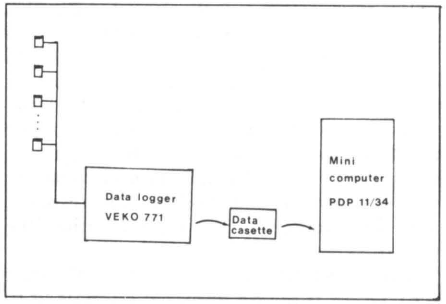

Fig. 3.2. Schematic representation of the Eos-system.

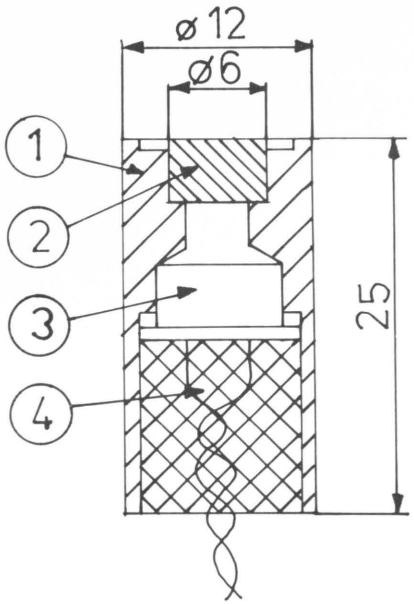

Fig. 3.3. Schematic representation of the construction of the sensor (1) PVC tube; (2) diffusing nylon plate; (3) photo cell PBW 21; (4) silicon glue. The scale is in mm. (Salminen et. al. 1983).

322. The data acquisition system

Data collection was carried out using a microprocessor-based, programmable VEKO 771 datalogger (Salminen and Ventilä 1979). When the number of sensors was less than twenty, the datalogger could measure each sensor every other second. Measurement of the sensors took one second (Salminen, personal communication). The datalogger used the intermediate second for output routines.

The logger transmitted the dated readings via a serial interface to a PDP 11/34 minicomputer in which a real-time data collection program (Lappi and Smolander 1981) performed logging and storage of the data onto disk storage.

323. The Eos system

The Eos system consisted of 32 light sensors and the datalogger programmed to carry out the following measurement procedure. Each sensor was measured in each measurement cycle and the results were grouped into

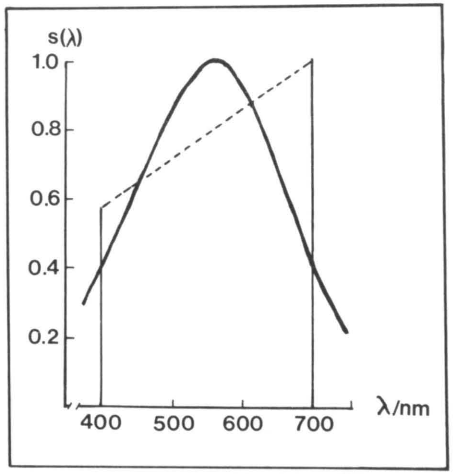

Fig. 3.4. Relative spectral sensivity, s, as a function of the wavelength of incoming radiation, λ, of the sensor (solid line) and that of an ideal quantum sensor (dotted line) (Salminen et. al. 1983).

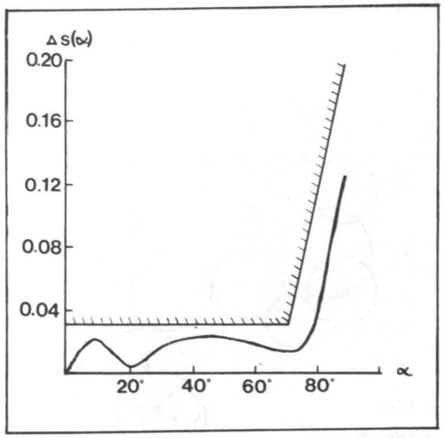

Fig. 3.5. Cosine error, Δs(α), of the sensor as a function of incoming angle, α. The curve is measured for a random sensor. The lines reject the area for the error curve of six randomly selected sensors (Salminen et al. 1983).

31 classes as shown in Table 3.1. The datalogger repeated the measurements 250 times at 2-second intervals and then recorded the dated distributions for each sensor onto a cassette. After this had been completed, the datalogger started a new 10 minute measurement cycle. It is thus possible to record the variation occurring simultaneously at 32 points during a period of 500 seconds.

33. The irradiance measurements and the study stands

331. Measurements of the time-space variation

The material concerning the time-space dynamics of radiation was collected in April 1981 in the experimental stand of the Primary Production Group, situated near to the Forest Field Station of the University of Helsinki (lat. 61° 51' N, long. 24° 17' E, elev. 160 m asl). The density of the stand was about 3 000 stems ha^{-1}, the mean height 5.3 m and the age about 20 years. The experiment plot was situated on a slight slope facing south. The location of the measuring array in the stand is shown in Fig. 3.6.

The thickness of the snow cover during the measurement period in April 1981 was about 80 cm. This caused problems in setting up the equipment and, for practical reasons, the sensor array had to be placed at a suitable working height of 90 cm above the snow surface. The sensor array was thus 170 cm above the ground surface. This was slightly below the mean crown bottom of the stand.

Table 3.1. Classification of the irradiance measured by each sensor.

Class	Class limits (W m^{-2})	Class	Class limits (W m^{-2})
1	0.0–0.9	17	31.6–39.7
2	1.0–1.2	18	39.8–50.0
3	1.3–1.5	19	50.1–63.0
4	1.6–1.9	20	63.1–79.3
5	2.0–2.4	21	79.4–99.9
6	2.5–3.1	22	100.0–125.8
7	3.2–3.9	23	125.9–158.4
8	4.0–4.9	24	158.5–199.4
9	5.0–6.2	25	199.5–251.1
10	6.3–7.8	26	251.2–316.1
11	7.9–9.9	27	316.2–398.0
12	10.0–12.5	28	398.1–501.1
13	12.6–15.8	29	501.2–630.9
14	15.9–19.9	30	631.0–794.2
15	20.0–25.0	31	794.3–999.9
16	25.1–31.5		

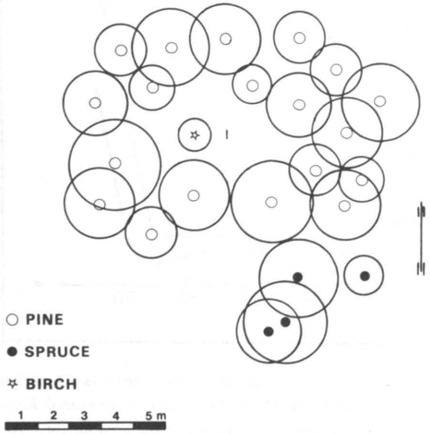

Fig. 3.6. Location of a 30-cm- long sensor array (bar) in the experimental stand (data sets A and B).

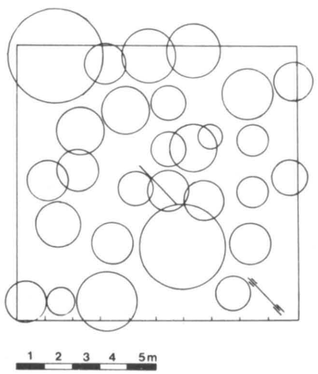

Fig. 3.7. Location of trees in the sample area in the Eos measurements (data set C). The location of the mast and the rods is depicted by the bar.

The sensor array was laid out horizontally in the north-south direction. In the first series of measurements (data set A) the sensor array consisted of 19 sensors at a spacing of 1.5 cm (the distance between sensors 15 and 16 was 3.0 cm), and in the second series (data set B), of 15 sensors at a spacing 3 cm. In addition, one sensor was placed above the nearby young plantation where the incoming radiation was recorded. The measurement periods of data set A and B and the prevailing weather conditions were as follows:

Data set	Measurement peiod	Day	Local time	Weather
A	1	14.4	14.06–14.39	Thick cloud cover
A	2	15.4	11.00–11.29	Sun obscured by thick clouds, occasionally sunny
A	3		13.04–13.30	Sunny
A	4		15.00–15.30	Hazy clouds. Direct sunlight at times
B	5	22.4	13.47–14.08	Cloudy, brief sunny periods
B	6		14.24–14.59	Sunny
B	7	23.4	12.28–13.10	Sun obscured occasionally by clouds

332. Temporal variation in different parts of the canopy.

In addition to the material described above, another material collected in July 1979 with the Eos system (Kellomäki and Oker-Blom 1983) was used to study the temporal variation, referred to as data set C. The density of the 18-year-old stand was 2 800 stems ha^{-1} and the mean height 3.8 m. The experimental plot sloped slightly to the south. The crown projections of the trees around the mast are presented in Fig. 3.7.

The sensors were arranged on rods located at heights of 4.3 (rod A), 2.97 (rod B), 1.64 (rod C) and 0.27 m (rod D). There were 4 sensors on the topmost rod, 8 sensors on the next, 12 on the second to the lowest, and 8 on the lowest one (Fig. 3.8). The location of the rods with respect to the vertical distribution of the stand biomass is shown in Fig. 3.9. The rods were placed in the north-south direction.

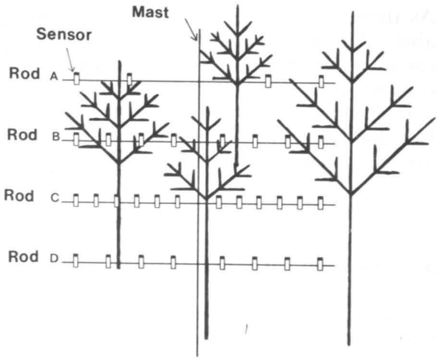

Fig. 3.8. Installation of thirty-two sensors of Eos system within the canopy (data set C).

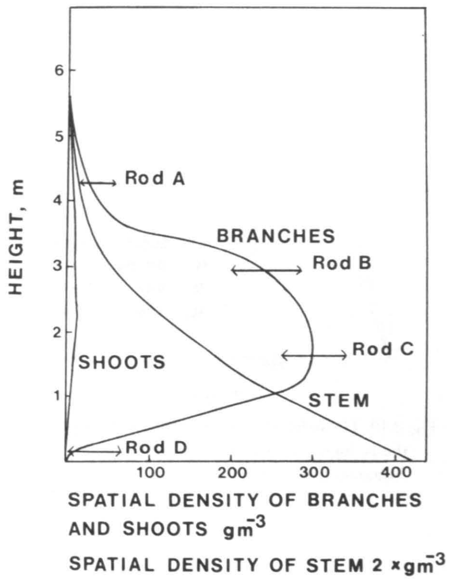

Fig. 3.9. Spatial density of the phytomass as a function of height. The heights of the rods and location with respect to the distribution of stand phytomass is depicted by bars.

As there was some shading woody biomass above the topmost rod, it was not possible to calculate the radiation variation above the canopy from the material. The measuring period lasted for 20 days but, owing to the fact that summer 1979 was rather wet, there are only a few sunny periods in the material.

34. The light response of photosynthesis

The significance of microvariation in the radiation for photosynthesis was studied by employing two, empirically determined light response curves of photosynthesis (Fig. 3.10). The low-curvature light response, later called the shoot light curve, was measured on a pine shoot, the stem of which was inclined at an angle of 45° with respect to the radiation beam. The length of the shoot was 9 cm, the needle angle 50°, the needle density 16 needles cm^{-1} and the mean needle length 4.9 cm. The high-curvature light response, later called the needle light curve, was measured on the same shoot, the stem being inclined at an angle of 90° with respect to the radiation beam. In addition, the needles whose inclination with respect to the radiation beam was not within the range 90 ± 10° were removed from the shoot in this case (for more details of the measuring technique, see Oker-Blom et al. 1983).

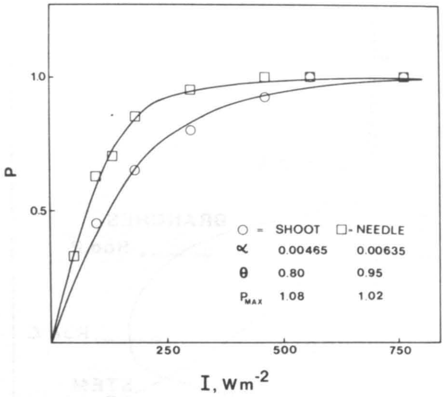

Fig. 3.10. The light response curve of the shoot photosynthesis (open circles) and the needle photosynthesis (squares) used in the calculations.

A non-rectangular hyperbola (Eq. 3.1, e.g. Thornley 1976) was used to describe the light response:

$$\theta P^2 - (\alpha I + P_{max})P - \alpha I P_{max} = 0 \qquad (3.1)$$

P = gross photosynthesis
I = irradiance
α = the initial slope of the light response curve
θ = the convexity parameter; when θ = 0 the curve is a Michaelis-Menten curve, and when θ = 1 the curve is a Blackman curve.
P_{max} = the saturation level of the photosynthetic rate

Relative values of photosynthesis were used in the computations, photosynthesis being given a unit value when the irradiance was 750 W m^{-2}. Parameters α, θ, and P_{max} in Eq. (3.1) were estimated iteratively using the criterion of least square sums. The light response curves and the values of the parameters of the non-rectangular hyperbola are presented in Fig. 3.10.

4. TEMPORAL MICROVARIATION

41. General

Passage of the sun across the sky results in regular variation in the incoming radiation but the variation is so slow that it is of no importance in photosynthesis measurements. On the other hand, movement of the clouds brings about large and rapid variation in the direct component of the incoming radiation. This variation is stochastic in nature. The variation in the diffuse radiation, as well as being small in amplitude, is also considerably slower. However, quantification of the frequency behaviour of the variation has been neglected in the ecological as well as in the meteorological research. On the other hand, variation in the mean irradiance during longer periods has been extensively studied (e.g. Mustachi et al. 1979).

The amplitude and frequency of the temporal variation at a certain point in a stand are often greater than in an opening because, in addition to the variation caused by the clouds, and movement of the foliage also cause variation. Andersson (1979) has found that the frequency of the variation in a maize field can be as much as 4 hz with an amplitude 80 % of the full irradiance. Detecting such a frequency would presuppose a sampling interval of as small as 0.125 seconds because the sampling frequency has to be at least double the frequency components of the phenomenon under study (Blackman and Tukey 1958).

The fluctuation of irradiance above and in the canopy is illustrated in Fig. 4.1 (data set A and B). It can be seen that the variation in the irradiance is occasionally rather large during cloudy periods above the canopy. The irradiance in the canopy is occasionally very labile. However, during periods of thick cloud cover the amplitude of the variation is small and the changes are slow. The temporal fluctuation is also very small during periods when the sensor is in the shade or, correspondingly, in sun flecks.

An attempt is made in the following to analyse the temporal variation by examining the distribution of the irradiance within periods of varying length (20–200 s). The distribution is depicted using standard deviation, the variation coefficient and skewness. In addition, the nature of the temporal microvariation is described by calculating the autocorrelation functions.

42. Variation during integration periods

Standard deviation of distributions: The frequency distributions of the standard deviations of the irradiance within periods of different length (20, 60, 100 and 200 s) are presented in Fig. 4.2 for the whole material (data sets A and B combined). The standard deviation distributions are extremely L-shaped. The maximum standard deviation during a 100-second period is 170 Wm^{-2} above the canopy, and 147 Wm^{-2} in the canopy. The median deviation is as small as 11 Wm^{-2} above the canopy, and 12 Wm^{-2} in the canopy. The within-period standard deviation increases strongly as the length of the period increases (Fig. 4.3). The mean standard deviation during a 20-second period is 13.6 Wm^{-2} above the canopy and 13.4 Wm^{-2} in the canopy, and during a 200-second period 49 and 39 Wm^{-2}, respectively.

The temporal variation of the irradiance in absolute values in the canopy was smaller than that above the canopy. This is due to the fact that the range of the variation in the irradiance is greater above the canopy than in the canopy. When the coefficient of variation is used to examine the relative variation, the relative variation is slightly greater in the canopy than above the canopy. The mean coefficient of variation for the 20-second period was 0.038 above the canopy, and 0.071 in the canopy (Fig. 4.4). The corresponding values for the 200-second period were 0.14 and 0.20. The maximum values of the coefficient of variation hardly change at all with respect to the length of the period, since the maximum value for the coefficient of varia-

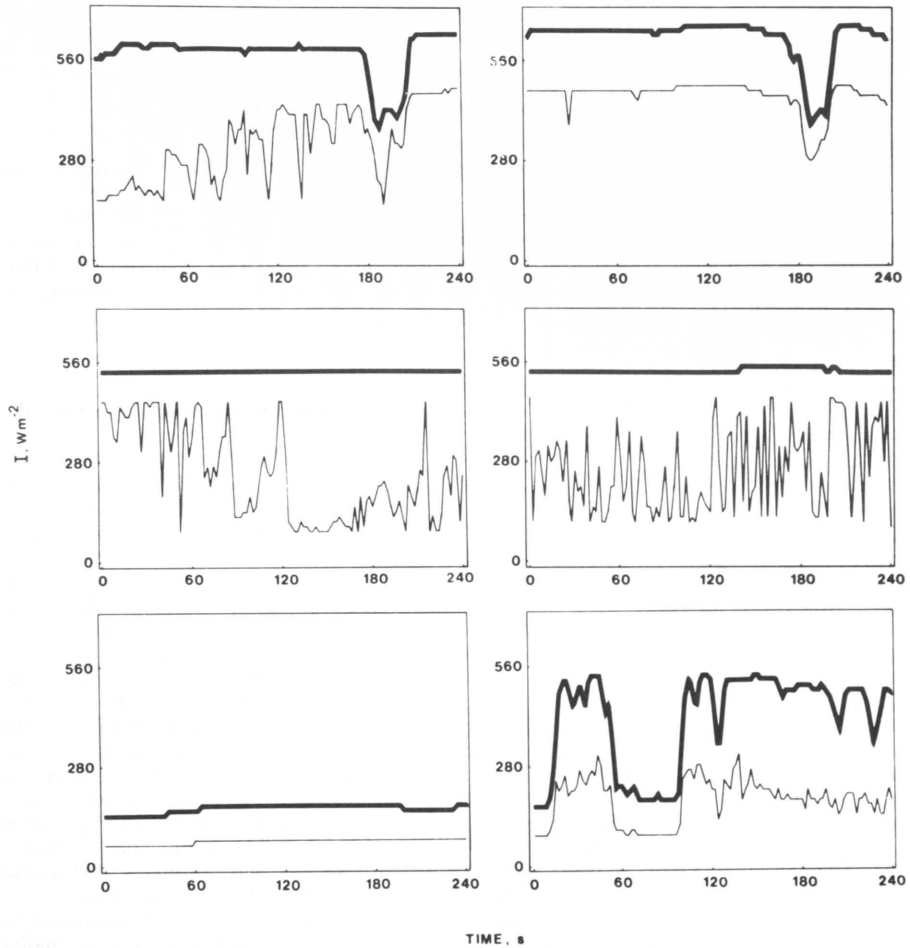

Fig. 4.1. Examples of temporal fluctuation of irradiance above the canopy (thick line) and within the canopy (thin line).

tion above the canopy was 0.52 during the 20-second period, and 0.51 during the 200-second period.

A theoretical maximum for the standard deviation can be calculated for each period as there is an absolute variation range for the irradiance. The maximum deviation is given by a two-point distribution with nonzero probabilities in the lower and upper limits, the mean of the distribution thus determining these probabilities. The maximum of the standard deviation is obtained using the formula, when $I_{min} = 0$:

$$\sigma_{max} = \sqrt{\bar{I}(I_{max} - \bar{I})} \qquad (4.1)$$

The actual standard deviation is usually considerably smaller than the theoretical

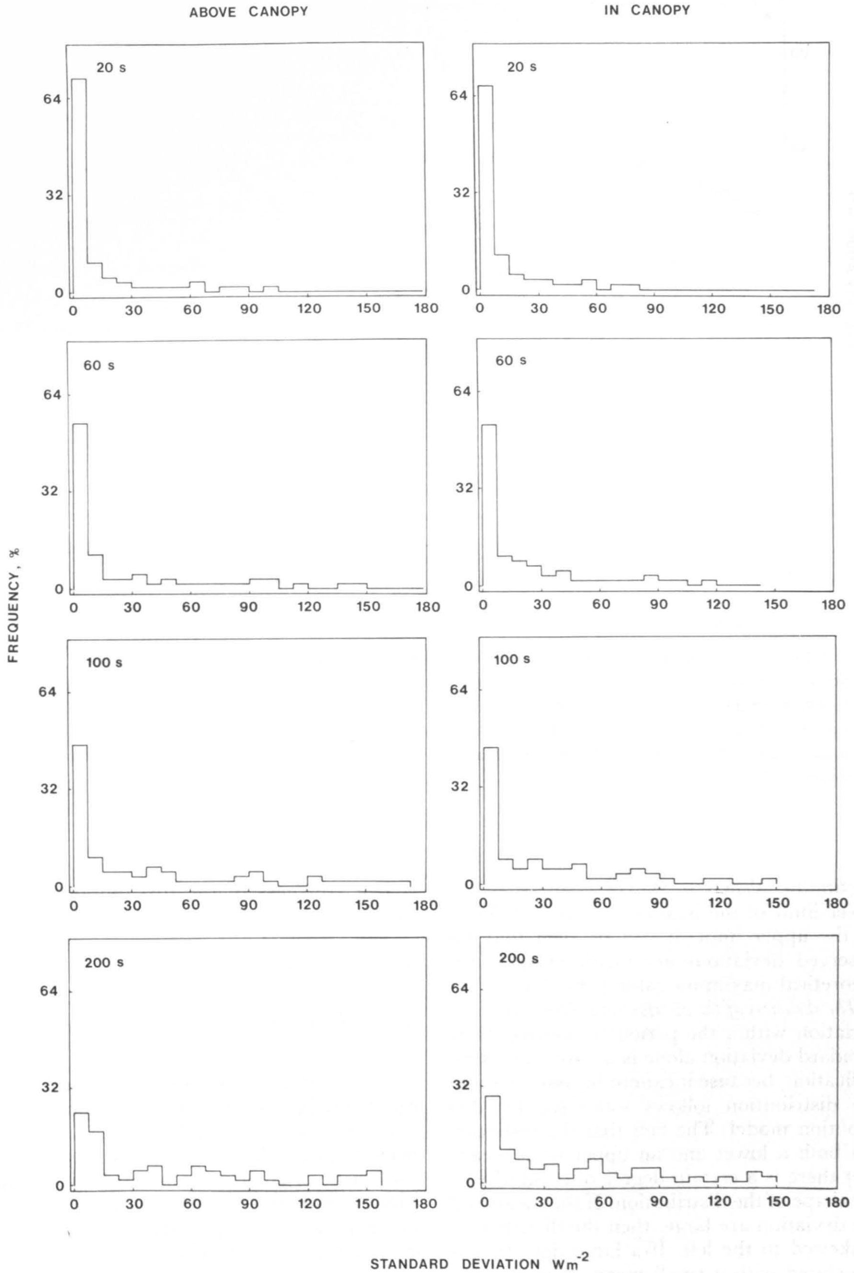

Fig. 4.2. The frequency distribution of the within-period standard deviations for periods of different length.

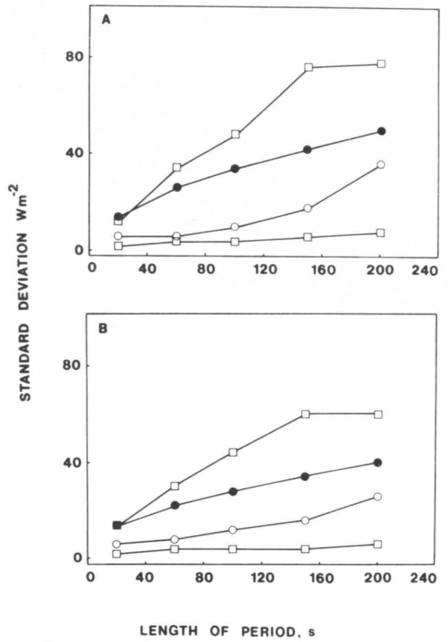

Fig. 4.3. Characteristics of the distributions of the within-period standard deviation as a function of the period length above the canopy (A) and within canopy (B). Lower and upper quartile plotted using open squares, the median as open circles and the mean as closed circles.

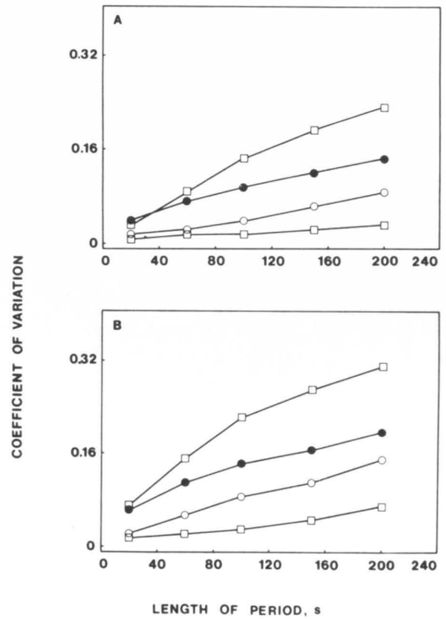

Fig. 4.4. Characteristics of the distributions of the within-period variation coefficient as a function of period length. Symbols same as in Fig. 4.3.

maximum. When 0 Wm^{-2} is used as the lower limit of the irradiance and 700 Wm^{-2} as the upper limit, it can be seen that the observed deviations are rarely close to the theoretical maximum value (Fig. 4.5).

The skewness of the distributions: Depicting the variation within the period by means of the standard deviation alone is a strong oversimplification, because it cannot be assumed that the distribution follows some regular distribution model. The fact that the radiation has both a lower and an upper limit means that there is a certain degree of regularity in the shape of the distribution. If the mean and the deviation are large, then the distribution is skewed to the left. If a large deviation is associated with a small mean, then the distribution is most likely skewed to the right.

The skewness of the distributions, G_1 is (see Snedecor and Cochran 1980):

$$G_1 = \frac{u_3}{\sigma^3}; \text{ where}$$

$$u_3 = \frac{1}{n} \cdot \sum_{i=1}^{n} (I_i - \bar{I})^3 \qquad (4.2)$$

The results for the 100-second period are presented in Fig. 4.6. The relationship between the skewness and the mean is as expected, although it is rather scattered. The coefficient of correlation is −0.42 above the canopy, and −0.48 in the canopy. The correlation is higher for periods with a standard deviation of over 30 Wm^{-2}. The correlation coefficient is then −0.79 above the canopy and −0.84 in the canopy. The existence of

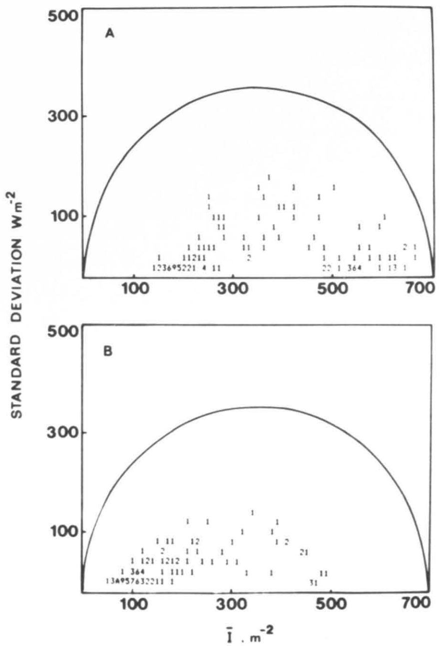

Fig. 4.5. The within 100-second period standard deviation and the calculated theoretical maximum standard deviation (Eq. 4.1, solid line) as a function of the mean irradiance above the canopy (A) and in the canopy (B). Symbols 1 through 9 refer to number of observations and A refers frequencies 10 . . . 19.

lower and upper limits affects the shape of the distribution only when the standard deviation is considerable. Thus even a larger mean can have a positively skewed distribution when the standard deviation is small.

Effect of weather type on the variation: The distributions for the whole material do not always correctly characterize the significance of microvariation, because the microvariation is very small both above and within the canopy when there is a thick cloud cover. The temporal microvariation is non-existent above the canopy during a sunny period. In the canopy, on the other hand, it is at times great. The variation is also noticeable above the canopy during cloudy periods. The frequency distributions for the within-period standard deviations during 20- second periods are presented in Fig. 4.7 for overcast, cloudy and sunny periods, and the characteristic values of the distributions for different types of weather in Fig. 4.8. Corresponding analyses with respect to the coefficients of variation are presented in Fig. 4.9.

During overcast weather, when the radiation is mainly diffuse and thus the temporal microvariation is very small, the mean deviation for a 20-second period was only 6.4 Wm^{-2} above the canopy and 2.9 Wm^{-2} in the canopy. During the cloudy periods, the features which generate and filter the temporal variation in the canopy compensate each

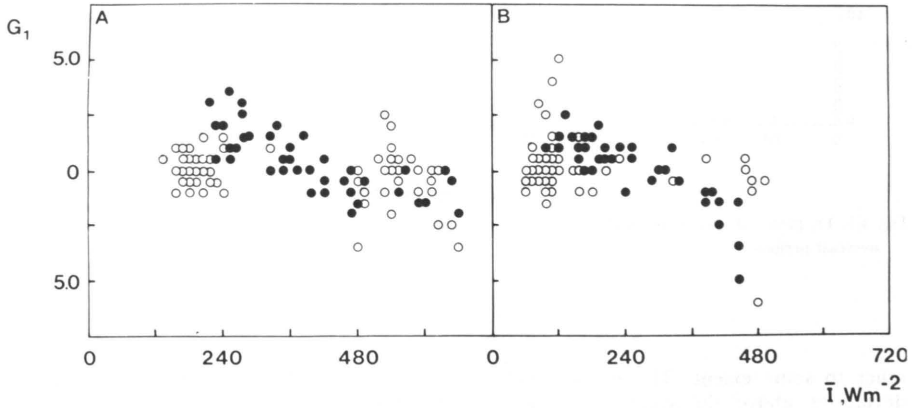

Fig. 4.6. The skewness of the within-periods distributions as a function of the mean irradiance above the canopy (A) and within the canopy (B). Periods of standard deviation less than 30 W/m^2 as open circles and more than 30 W/m^2 as closed circles.

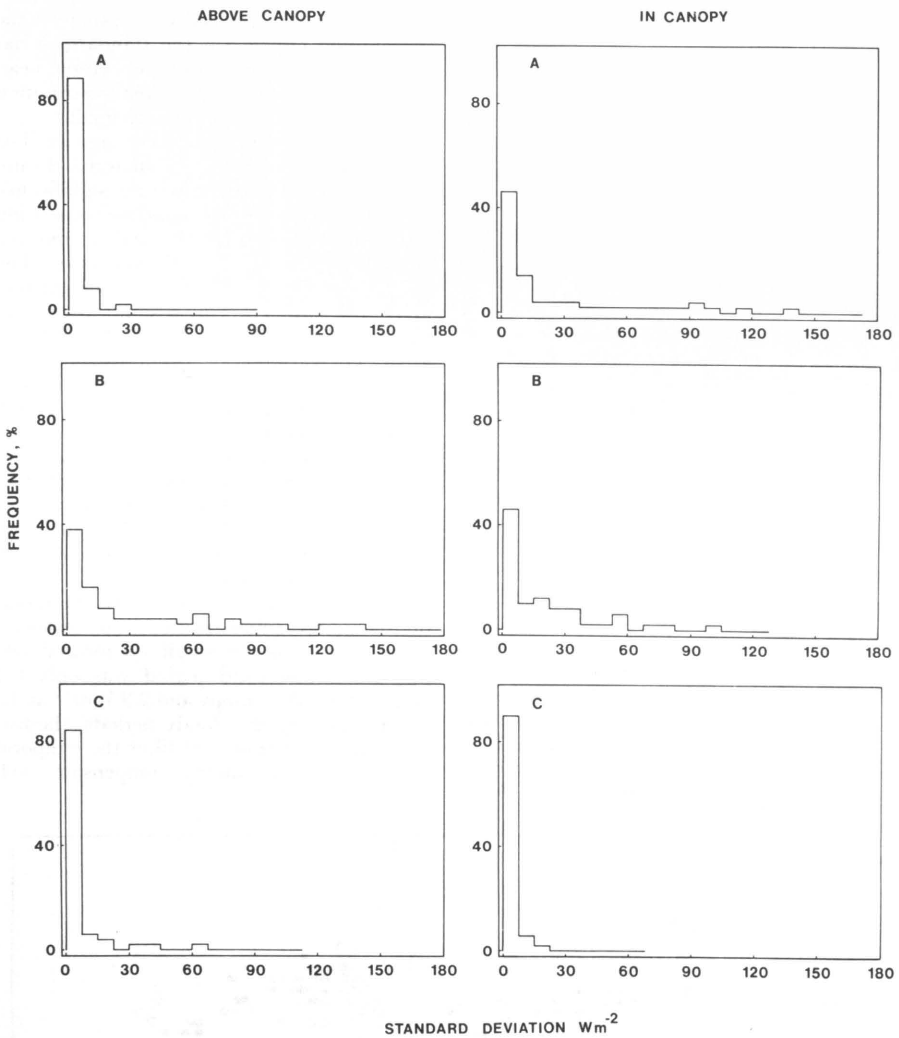

Fig. 4.7. Frequency distributions of the standard deviations within 20-second periods. A sunny, B cloudy and C overcast periods

other to some extent. The mean standard deviations above the canopy and in the canopy were of the same order of magnitude: the deviation above the canopy was 33 Wm^{-2} and in the canopy 20 Wm^{-2}. During sunny periods, when the variation in the incoming radiation was insignificant (5 Wm^{-2}), the temporal microvariation caused by the canopy was considerable, 30 Wm^{-2}.

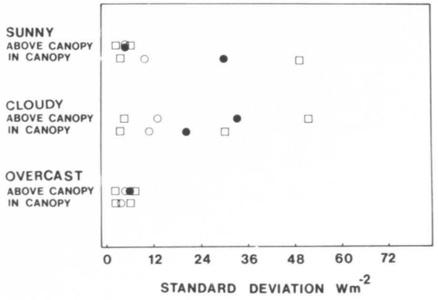

Fig. 4.8. Characteristics of the frequency distributions of within-periods standard deviation in different weather types. Symbols same as in Fig. 4.3.

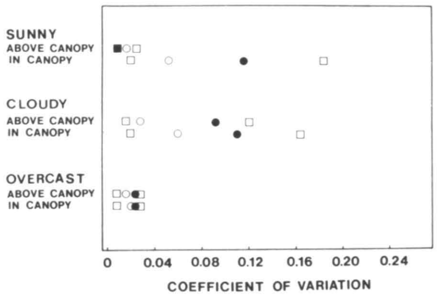

Fig. 4.9. Characteristics of the distributions of the within-period variation coefficient in different weather types. Symbols same as in Fig. 4.3.

43. Variation in different parts of the canopy

Vertical transect: Because the spatial and temporal representability of data sets A and B was poor, the temporal microvariation will be examined on the basis of data set C. This material consists of frequency distributions of irradiance collected during periods of 500 seconds at 4 different heights on a total of 20 days. Variation analyses were carried out separately for overcast, cloudy and sunny periods. The overcast period comprises data for one day, the cloudy period for three days, and the sunny period consists of data for two mornings (6.00–11.30 h).

The distributions of the within-period standard deviation at different heights are presented side by side for the different types of weather in Fig. 4.10. The distribution for each height is formed from the sum of the distributions of all the sensors at the height in question. The characteristics of the distributions are presented as a function of height in Fig. 4.11. The corresponding analysis carried out using the coefficients of variation is presented in Fig. 4.12.

The within-period standard deviation increased with respect to height at all weather types. The differences between weather types were rather small in the lower part of the canopy. This is presumably due to the high proportion of diffuse radiation and its temporal stability in comparison to direct radiation. The temporal variation is greatest during cloudy periods. The relative deviation decreases with increasing height during overcast or sunny periods, but during the cloudy period the coefficient of variation decreased gently as the height of the sensor rod increased.

Horizontal transect: The mean irradiance during longer periods (e.g. one day) has been found to be rather stable in a horizontal plane in a number of different types of vegetation cover (e.g. Anderson 1966). This principle of horizontal homogeneity has also been applied to pine stands (Hari et al. 1982a). The daily mean radiation on a horizontal plane in the pine stand of the present study varied very much, however, during all the weather types (Fig. 4.13). When measured in absolute units, the variation in the mean irradiance was greatest in the middle of the canopy (h = 3.0 m) during sunny weather. In this case the difference between the highest and lowest mean irradiance was as much as 185 Wm^{-2}. The point with the greatest illumination received 2.6 times as much radiation as the most shaded one at the same height.

In relative terms, the horizontal heterogenity is of the same order of magnitude during the other weather types. Even on an overcast day when most of the radiation is diffuse, the differences are rather large. At a height of 3.0 m the point receiving the most radiation recorded an irradiance of 96 Wm^{-2} and the most shaded point 49 Wm^{-2}. In other words,

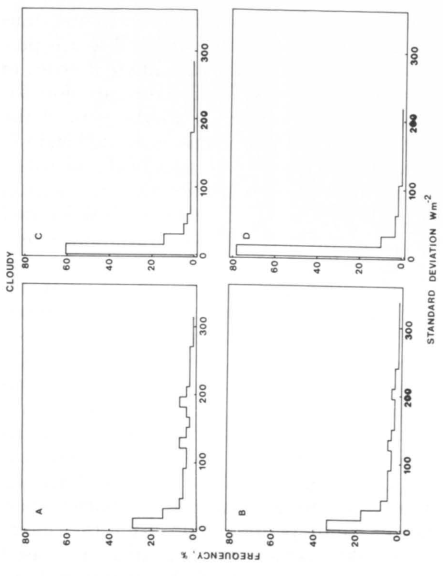

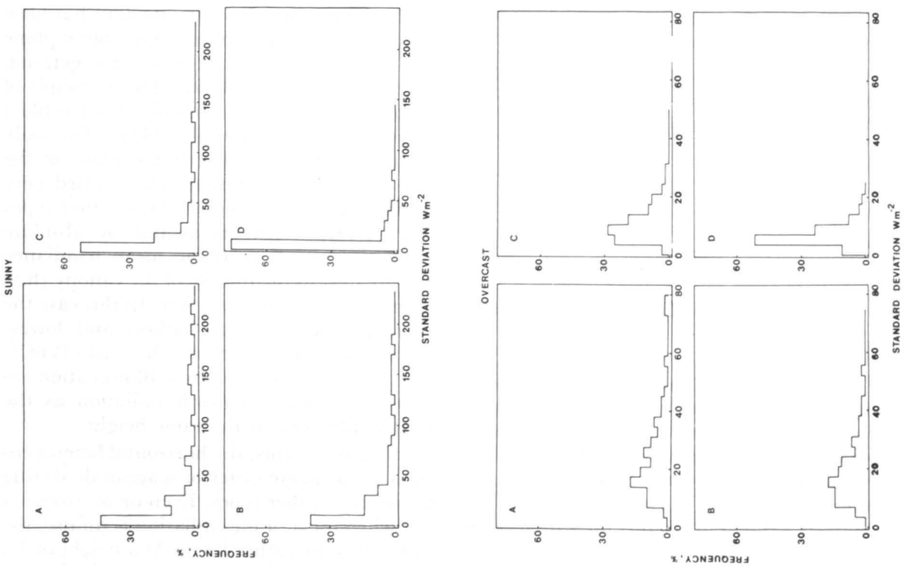

Fig. 4.10. Frequency distributions of the within 500-second period standard deviations at different rod heights and during different types of weather. A h=4.30, B h=2.97, C h=1.64 and D h=0.27 m.

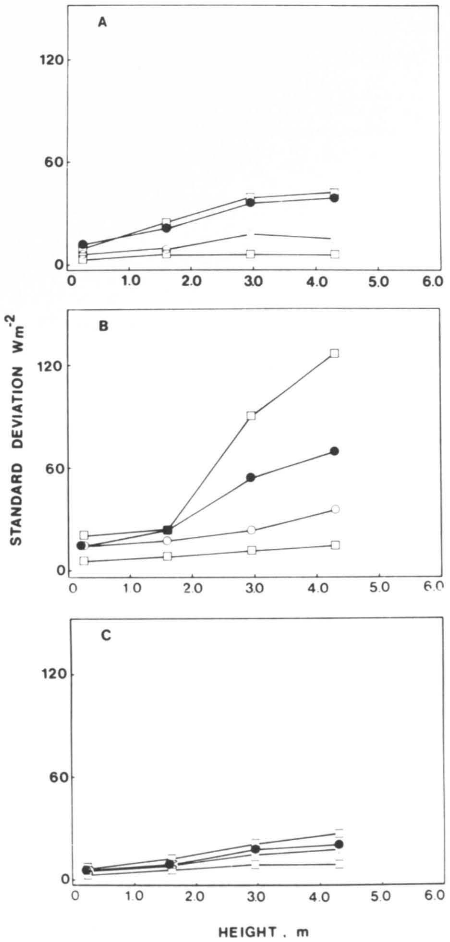

Fig. 4.11. Characteristics of the frequency distributions for the within 500-seconds periods standard deviations as a function of rod height on sunny (A), cloudy (B) and overcast (C) days. Symbols are the same as in Fig. 4.3.

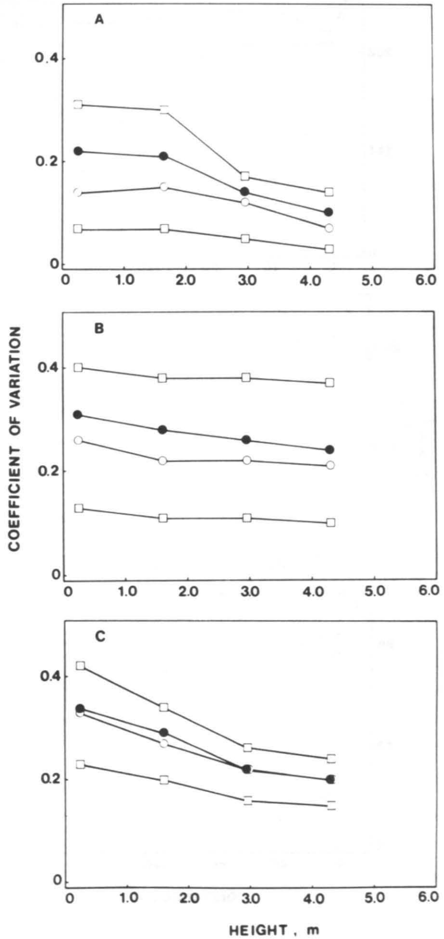

Fig. 4.12. Characteristics of the frequency distributions for the within 500-second period variation coefficient as a function of rod height. Symbols are the same as in Fig. 4.3.

almost twice as much radiation falls on the most illuminated point as on the most shaded one.

The within-period standard deviation behaves in a very similar way to the mean irradiance (Fig. 4.14), although it is not as regular. The deviation is largest at points where the mean irradiance is greatest. The largest differences in the mean standard deviation are of the order of 30 Wm^{-2}. The largest mean standard deviation is in this case almost three times that of the smallest mean

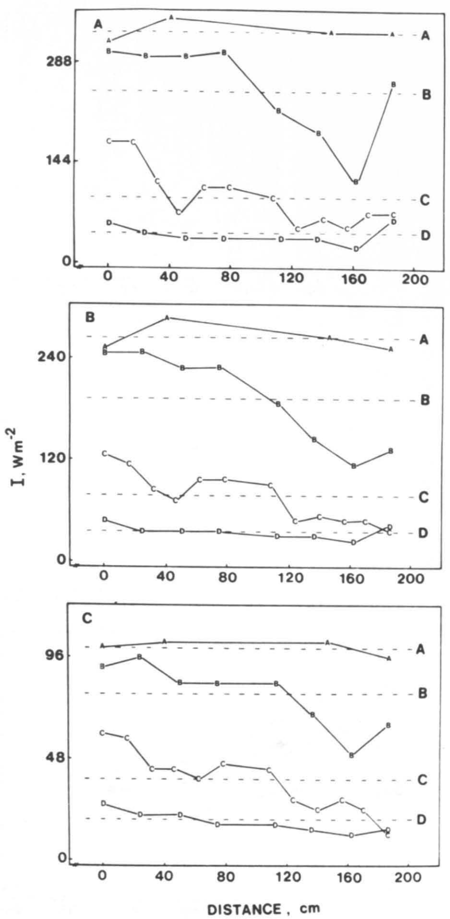

Fig. 4.13. Transects of the mean irradiance at different rod heights. A sunny, B cloudy and C overcast days.

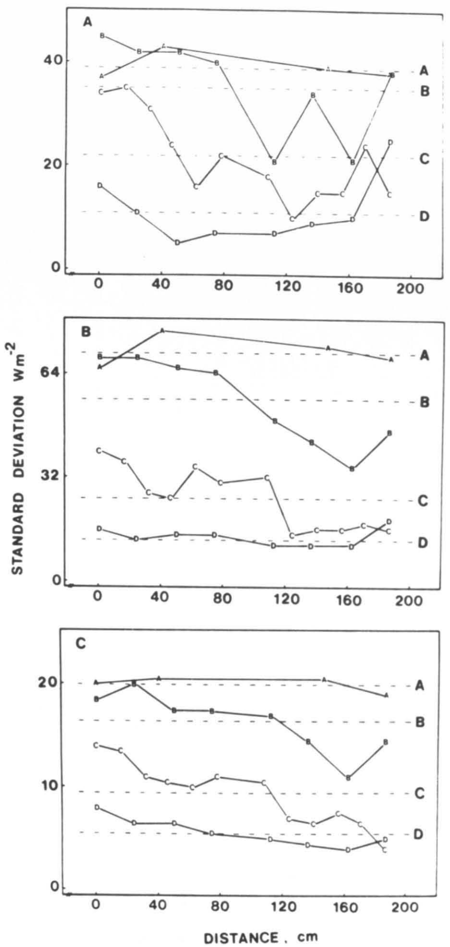

Fig. 4.14. Transects of the mean within 500-second period standard deviations.

standard deviation at the same level. The behaviour of the within-period coefficient of variation is considerably more stable in the horizontal plane during overcast weather, but during sunny weather the horizontal variation is still great even when examined with the coefficient of variation (Fig. 4.15).

Spatial heterogeneity: The deviation analyses done with data set C showed that the temporal microvariation of irradiance fluctuates over a wide range in the different parts of the canopy. The heterogenity is significant in both the vertical and the horizontal direction and hence the results of data sets A and B cannot be extrapolated to different heights of the canopy, and even the horizontal generalization is very poor.

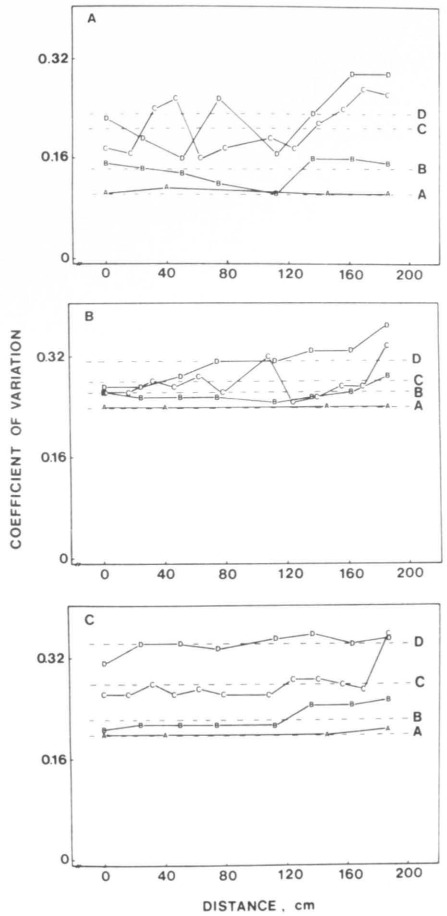

Fig. 4.15. Transects of the mean within 500-second period variation coefficient.

44. Serial autocorrelation

In the following, the nature of the temporal microvariation is examined by means of the serial autocorrelation. The autocorrelation function provides information about how the independence of the measurements increases as the time between the measurements lengthens. The autocorrelation functions were calculated from the irradiance and also from the relative irradiance (irradiance in canopy/irradiance above canopy). The time lag varied between 0–200 seconds in the calculation of the autocorrelation functions.

The autocorrelation functions for different measuring periods are presented with respect to the time lag in Fig. 4.16. The irradiance within and above the canopy is plotted against the lagged irradiance for different lag values in Fig. 4.17. The behaviour of the autocorrelation functions is rather stable with respect to the time lag. However, the functions for the different periods are very different in type. In addition, the relationships between the different functions (irradiance above the canopy, irradiance in the canopy and the relative irradiance) are not regular. Thus the irradiance in the time scale examined here cannot be considered to be a stationary random process. Instead its "nature", as the variation in the shape of the autocorrelation functions shows, varies according to the position of the sun, the cloud cover and the wind. If the irradiance would be a first order Markov process, then the autocorrelation function would decrease exponentially with respect to time (e.g. Barlett 1966).

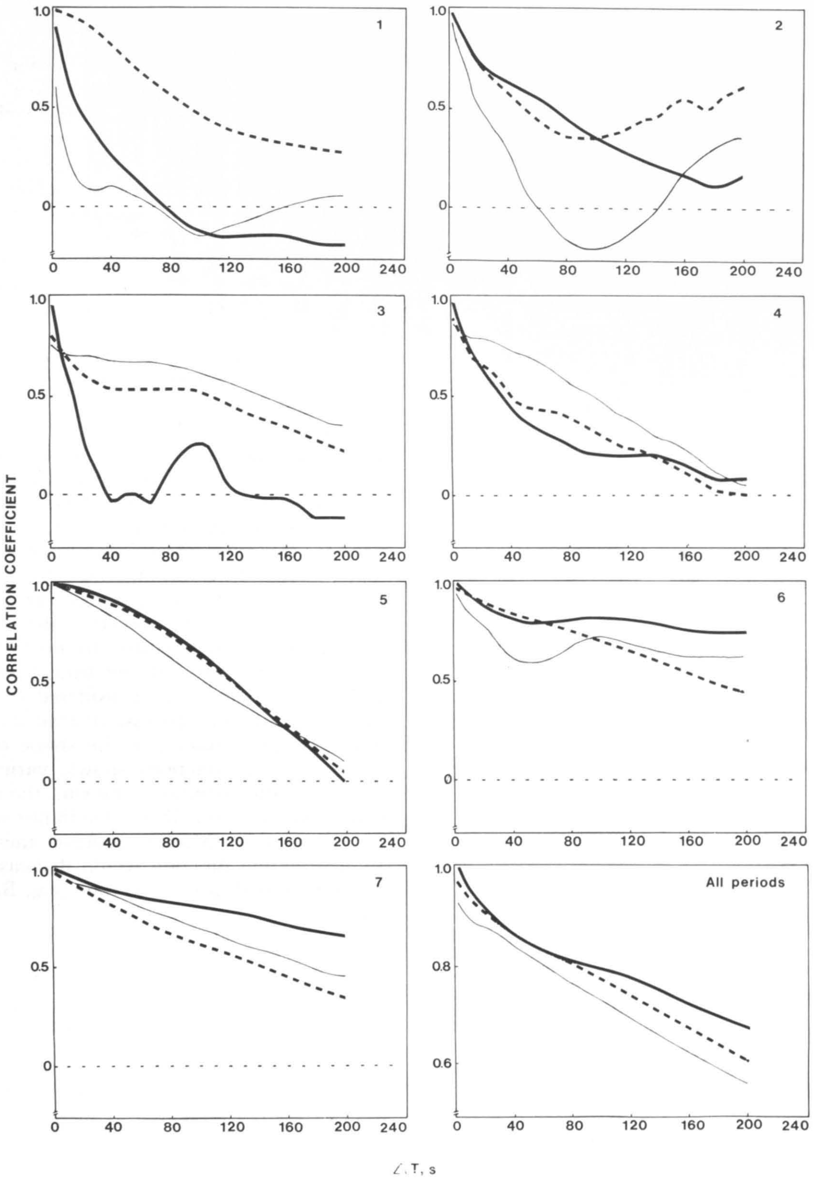

Fig. 4.16. Serial autocorrelation functions of the measurement periods 1–7, the time lag being varied between 0–200 s. Thick line for irradiance above canopy, thin line for irradiance in the canopy and broken line for relative irradiance.

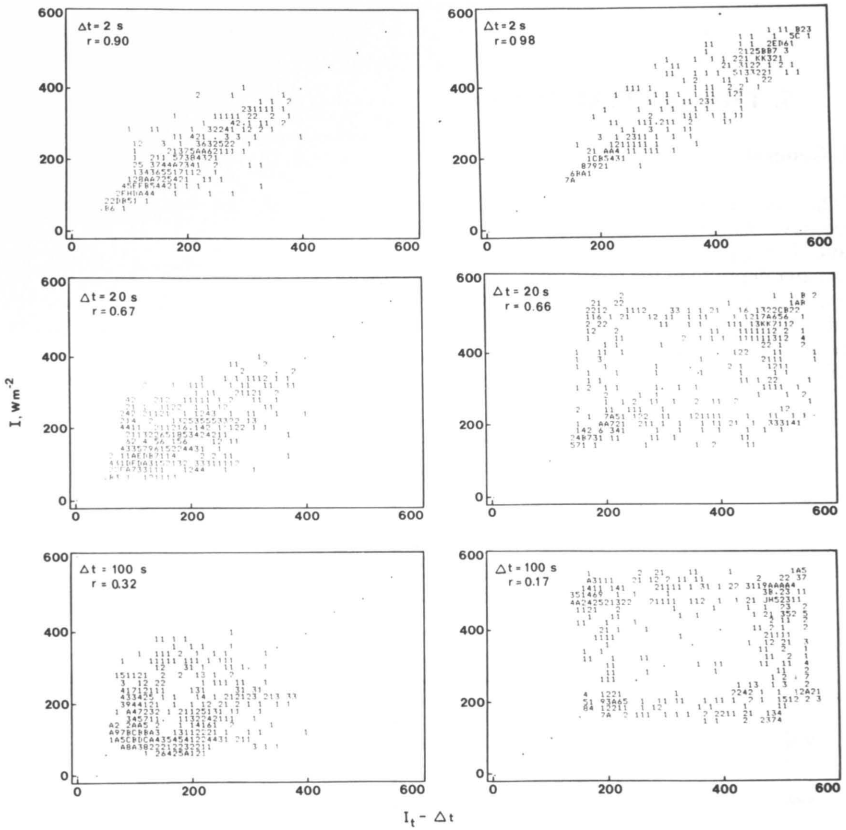

Fig. 4.17. Irradiance above (on the right) and within (on the left) canopy as a function of lagged irradiance for lag values of 2, 20 and 100 s. Symbols 1 through 9 refer to the number of observations, A refers to frequencies 10 . . . 19, B 20 . . . 29 and P more than 160.

5. THE SPATIAL MICROVARIATION IN THE CANOPY

51. General

The instantaneous irradiance in the canopy varies very strongly in the horizontal plane. This type of variation has been studied in greater depth than the temporal microvariation, because it is the central problem in studies concerning the architecture of the canopy (e.g. Niilisk et al. 1970, Acock et al. 1970).

The spatial microvariation has been studied by visually estimating, using Lopukhin's rod, the relative proportion of sun flecks (ref. Ross 1981). Another method is to scan the transect using a light sensor, and either a fast strip recorder (Niilisk et al. 1970) or a mass memory (Norman and Tanner 1969) for storing the data.

The nature of the spatial microvariation is illustrated in Fig. 5.1 by drawing various

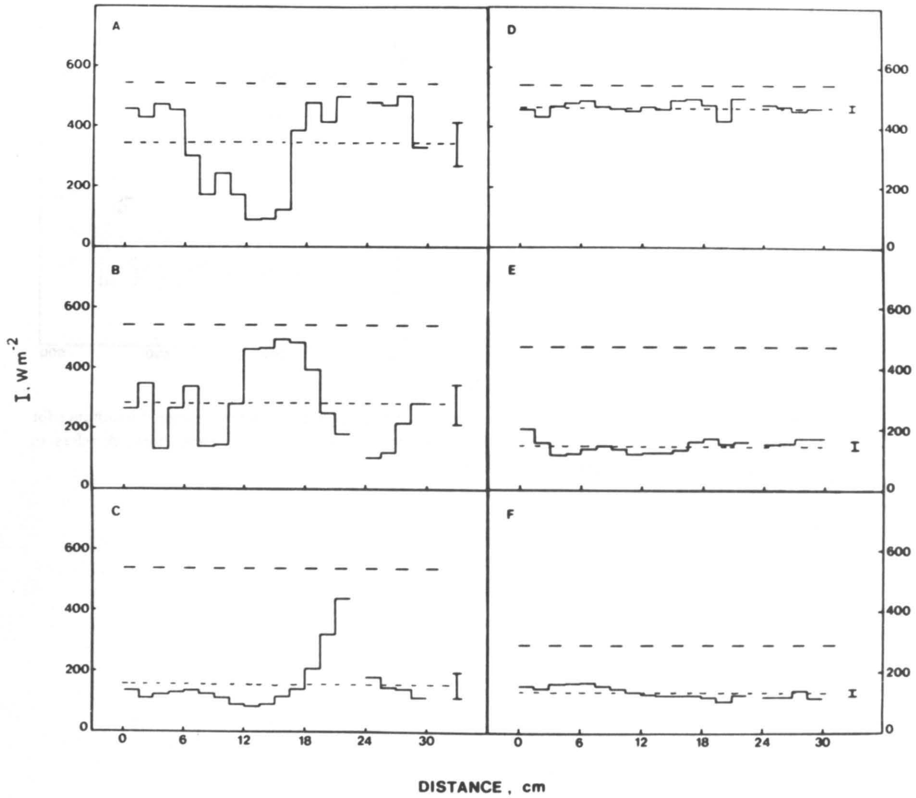

Fig. 5.1. Examples of horizontal transects of irradiance (solid line), irradiance above the canopy (broken line), mean irradiance within canopy (dotted line) The bars indicate the standard deviation. Transects A, B and C are measured every 2nd second.

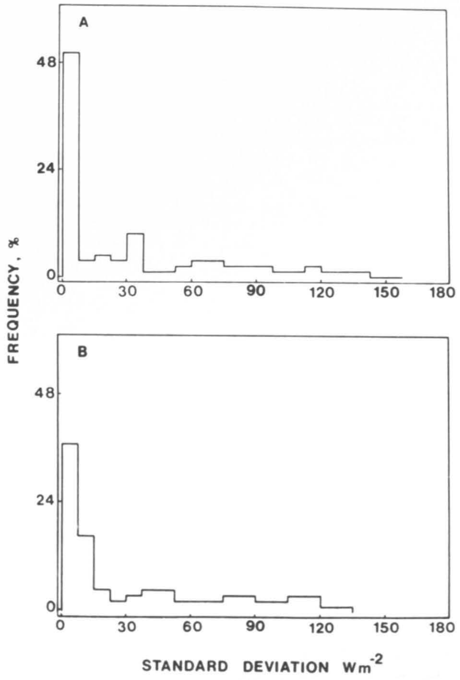

Fig. 5.2. Frequency distribution of the within-distance standard deviation in data set A and B.

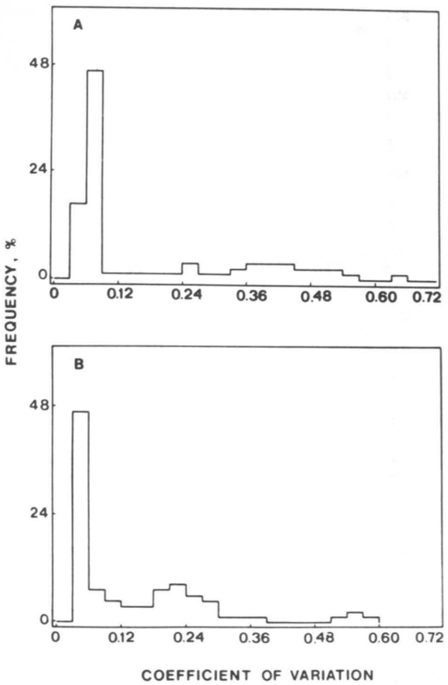

Fig. 5.3. Frequency distribution of the within-distance variation coefficient in data set A and B.

horizontal transects. The profiles are low when there is a thick cloud cover, but during cloudy and sunny weather the profile is occasionally very variable.

52. Variation on the horizontal plane

The frequency distributions of the within-distance standard deviations are presented in Fig. 5.2. The median standard deviation in data set A, where there were 19 sensors spaced at intervals of 1.5 cm, was 7.3 Wm^{-2}, and in data set B, where there were 15 sensors at 3.0 cm spacing, it was 13.2 Wm^{-2}. The standard deviation distributions in both materials are extremely L-shaped, which depicts the large proportion of the small variation in such conditions. The median of the coefficient of variation in data set A was 0.008 and 0.07 in data set B (Fig. 5.3).

The situation changes essentially when the distribution is examined separately for each type of weather (Fig. 5.4). The distribution of the sunny periods is peaked when the mode is of the order of 70 Wm^{-2}. The median standard deviation during a sunny period is 66 Wm^{-2} in data set A, and 17 Wm^{-2} during a cloudy period. When there is a thick cloud cover, i.e. all the radiation is diffuse, the deviation with respect to space is extremely small, the median being only 5.7 Wm^{-2} in data set A. The upper quartile of the sunny period was 74 Wm^{-2}, in the cloudy period 44 Wm^{-2} and in the overcast period 6.3 Wm^{-2}.

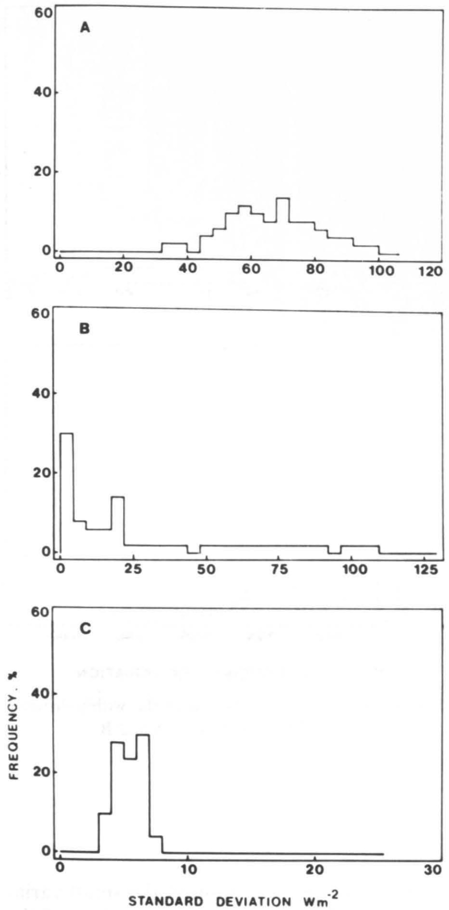

Fig. 5.4. Frequency distributions of within-distance standard deviation during different types of weather. A sunny, B cloudy, C overcast.

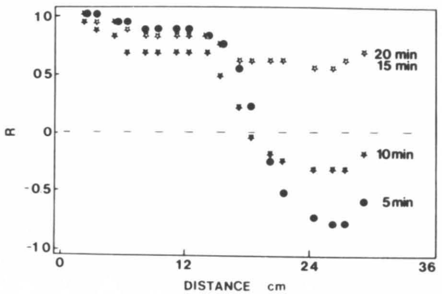

Fig. 5.5. Deformation of the spatial autocorrelation function with increasing time period.

53. Spatial autocorrelation

The spatial microvariation is characterized in the following by means of the autocorrelation functions. Norman and Tanner (1969) have used the autocorrelation technique for describing the microvariation. Nilson (1971) has used Markov's chain for characterizing the vertical behaviour of light.

Autocorrelation analysis can also be done with respect to space for the relative irradiance (irradiance in the canopy/irradiance above the canopy). The variation in the irradiance above the canopy is thus not included in the correlation coefficient.

It was found that the passage of the curves varied very much in different periods. This was especially the case when the autocorrelation functions were calculated for short periods. The development of the autocorrelation function as the length of the period under examination increases, is illustrated in Fig. 5.5. The effect of the structure of the canopy is clearly evident in the curve for the short period, since the correlation coefficient does not decrease uniformly and becomes negative after a distance of 18 cm ($R_{min} = -0.79$). As the length of the period under study increases, the variation due to the structure of the canopy decreases and the graph becomes more stable. The autocorrelation functions for different measuring periods are presented in Fig. 5.6. The correlation diagrams for different distances between the sensors are depicted in Fig. 5.7.

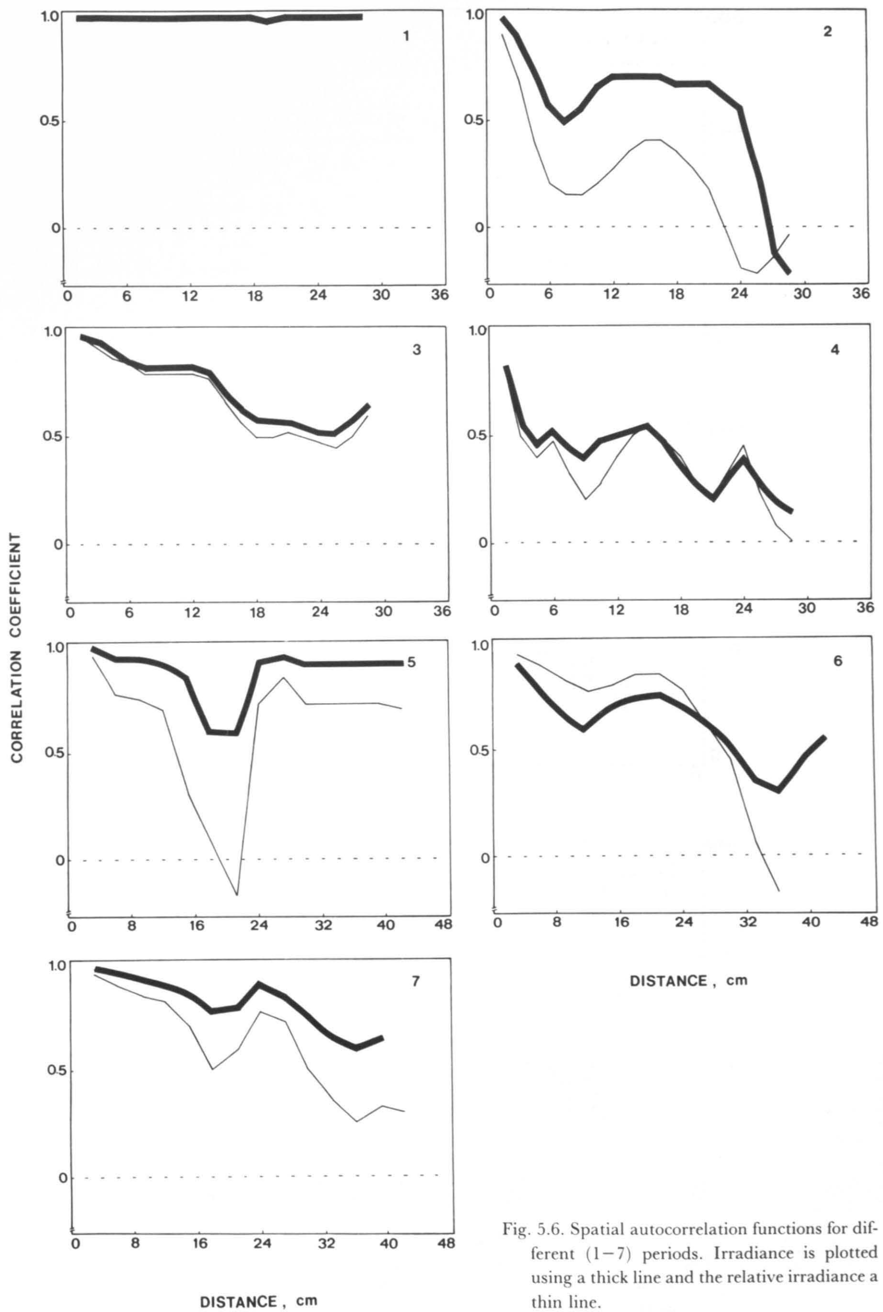

Fig. 5.6. Spatial autocorrelation functions for different (1–7) periods. Irradiance is plotted using a thick line and the relative irradiance a thin line.

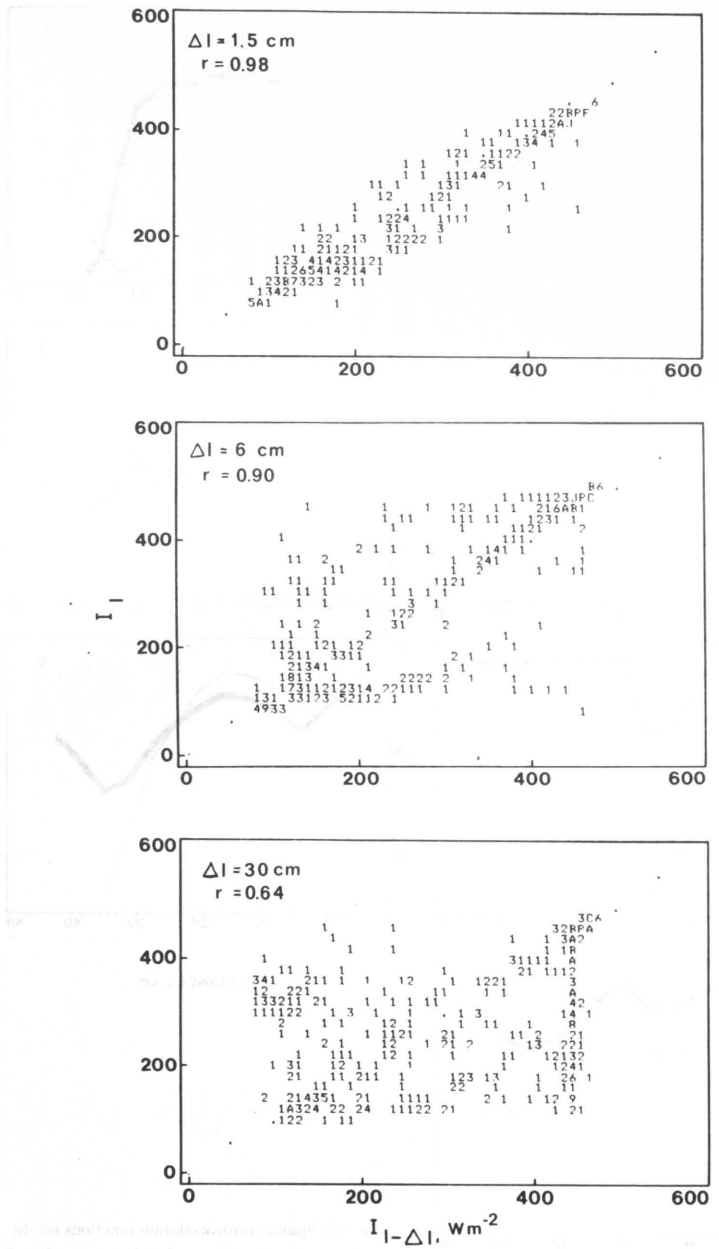

Fig. 5.7. The correlation between irradiance and lagged irradiance within the canopy for lag values 1.5, 6.0 and 30.0 cm. Symbols are the same as in Fig. 4.17.

6. COMPARISON OF THE APPROXIMATION METHODS

61. Linear approximation

611. Integration over time

The error above the canopy: The estimate of photosynthesis based on linear approximation, $\hat{P}_L$, and its error, ε_L, are presented with respect to "true photosynthesis" $\bar{P}$ in Fig. 6.1. for the whole measuring period above the canopy. The integration time is 100 s, and the light curves for the shoot and for the needles are used as the light response of photosynthesis. The error is at its greatest when the value of $\bar{P}$ is between 0.7 and 0.8. The maximum error for both curves is 7 % of the value of P_{max}. The absolute error $(100 \cdot \varepsilon_L / P_{max})$ is used in this study instead of the relative error $(100 \cdot \varepsilon_L / \bar{P})$. If one wants to emphasize the severity of possible errors, large error figures can be obtained for small values of $\bar{P}$ by using relative errors (cf. Hari et al. 1984).

The frequency distributions of ε_L for both the shoot and the needle light curves is presented in Fig. 6.2. The frequency distributions are extremely L-shaped. The median of ε_L is 0.06 % for the shoot light curve and 0.07 % for the needle light curve. The means are 0.67 % and 0.42 % respectively.

The error in the canopy: The error due to linear approximation within the canopy is examined in the following on the basis of the observations made with sensor No. 1. This sensor was in the same position in both data sets. Although the temporal microvariation

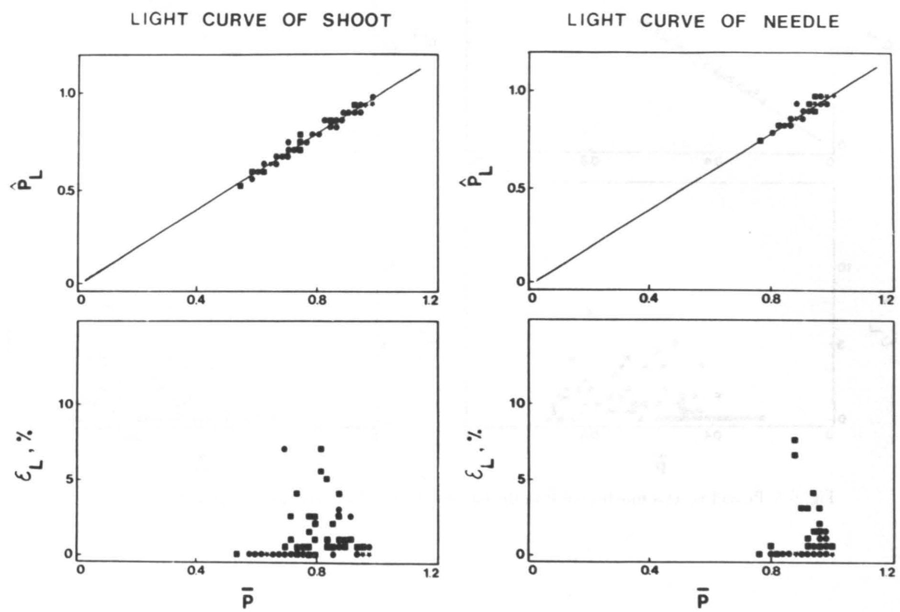

Fig. 6.1. $\hat{P}_L$ and ε_L as a function of $\bar{P}$ above canopy. Frequencies less or equal to 5 as squares and greater than 5 as circles.

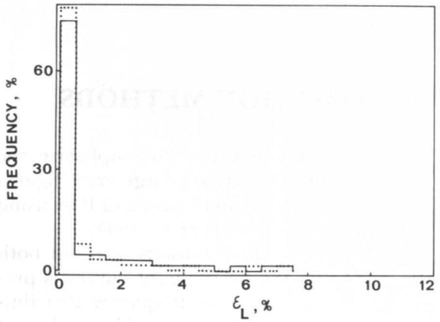

Fig. 6.2. Frequency distribution of ε_L in the open. The solid line represents the light response of the shoot photosynthesis and dotted line the needle light response.

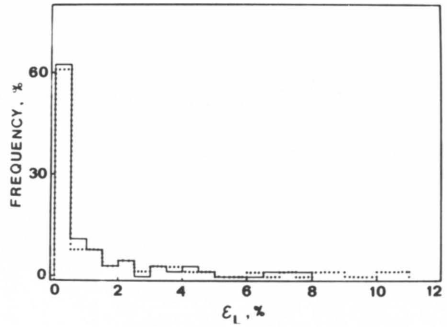

Fig. 6.4. Frequency distribution of ε_L in the canopy. The solid line represents the photosynthetic light response of the shoot and dotted line the needle light response.

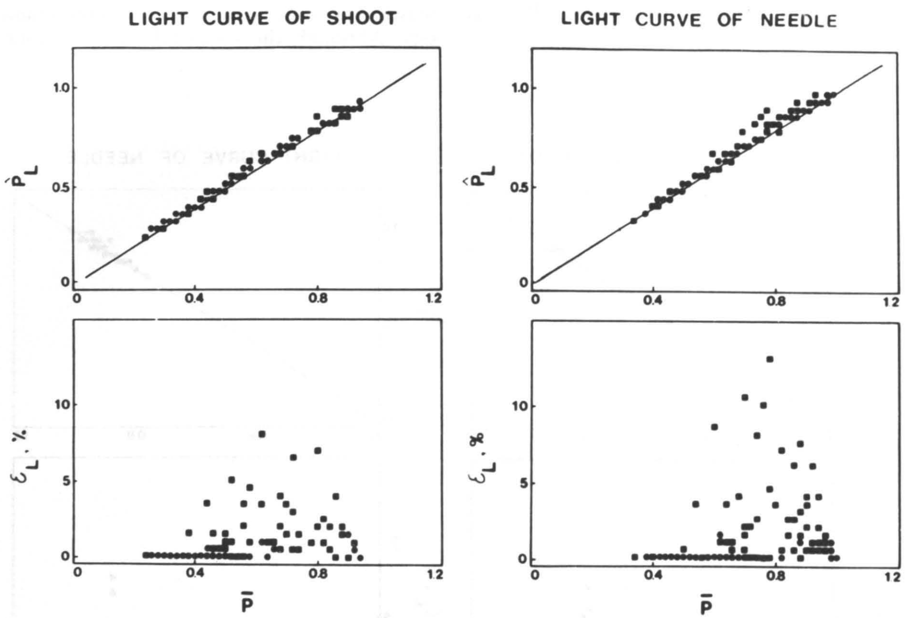

Fig. 6.3. $\hat{P}_L$ and ε_L as a function of $\bar{P}$ in the canopy. Symbols are the same as in Fig. 6.1.

was smaller within the canopy than above the canopy, linear integration gave a poorer result for both light curves in the canopy (Fig. 6.3 and 6.4). The median error is 0.1 % both for the shoot and needle light curves. The mean values are 0.82 % and 1.27 %, and the observed maximum errors 7.8 % and 12.9 % respectively.

Thus, despite the smaller temporal microvariation, linear integration gives a poorer result in the canopy than in the open for both light curves. In addition, the needle light curve clearly gives a poorer result in the canopy. Both these features can be explained by the fact that a greater proportion of the variation in the canopy was within the saturated region of the light curve than above the canopy, where most of the observations were in the saturated area. From the point of view of practical measurements, however, the error is in most cases rather small because even in the case of the needle light curve, 75 % of the errors were below 1 % of the value of P_{max}.

Sensitivity to integration time: As the length of the measuring period increases, so does the variance within the period (Section 4), and through this also the error due to linear approximation ε_L. The effect of the length of the integration period on the error is examined in the following. Characteristics of the ε_L distributions with respect to the integration time are presented in Fig. 6.5. The integration time varies between 20 and 200 s and the shoot light curve is used as the light response. In this material the integration time did not have any essential effect on the magnitude of the observed maximum error. The maximum error above the canopy is smallest (6.2 % of the value of P_{max}) with a period of 20 s, and greatest (7.4 %) with a period of 100s. The largest value (9.28 %) in the canopy was obtained with an integration time of 20 s, and the smallest value (7.8 %) with a period of 100s. On the other hand, the other parame-

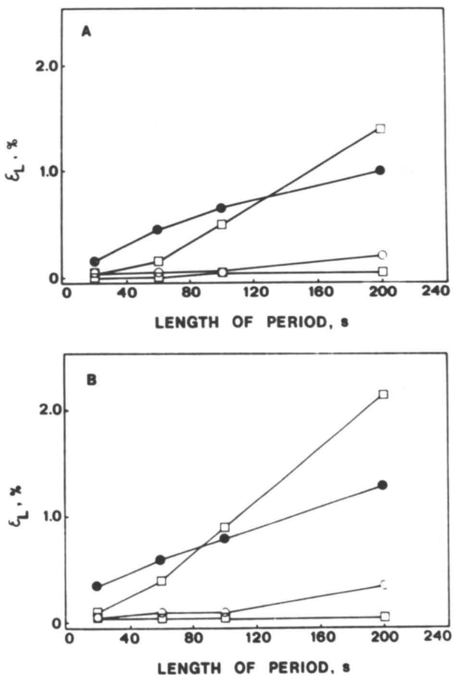

Fig. 6.5. Characteristics of the distribution of ε_L as a function of the length of the integration period above the canopy (A) and within the canopy (B). Symbols are the same as in Fig. 4.3.

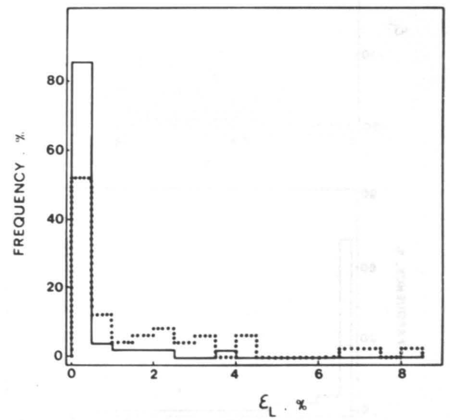

Fig. 6.6. Distribution of ε_L in the canopy for a 20 s integration period (continuous line) and for a 200 s integration period (dotted line).

ters of the distribution of the error show that the error increases strongly as a function of the integration time. Above the canopy, the upper quartile increases by a factor of 25 and the mean by a factor of 6 when the integration time increases from 20 to 200 s. The corresponding values for within the canopy are 22 and 4. The distribution of the error becomes more and more L-shaped as the integration time is shortened (Fig. 6.6).

In photosynthesis measurements, a measuring period of 200 s is far too long for a so-called clap-type cuvette because the cuvette will heat up considerably (e.g. Lange 1962). It is thus evident that linear integration will give reasonable results in photosynthesis measurements in the open. The error in the canopy is also moderate, especially when short integration times are used. This is in agreement with the experience gained by the

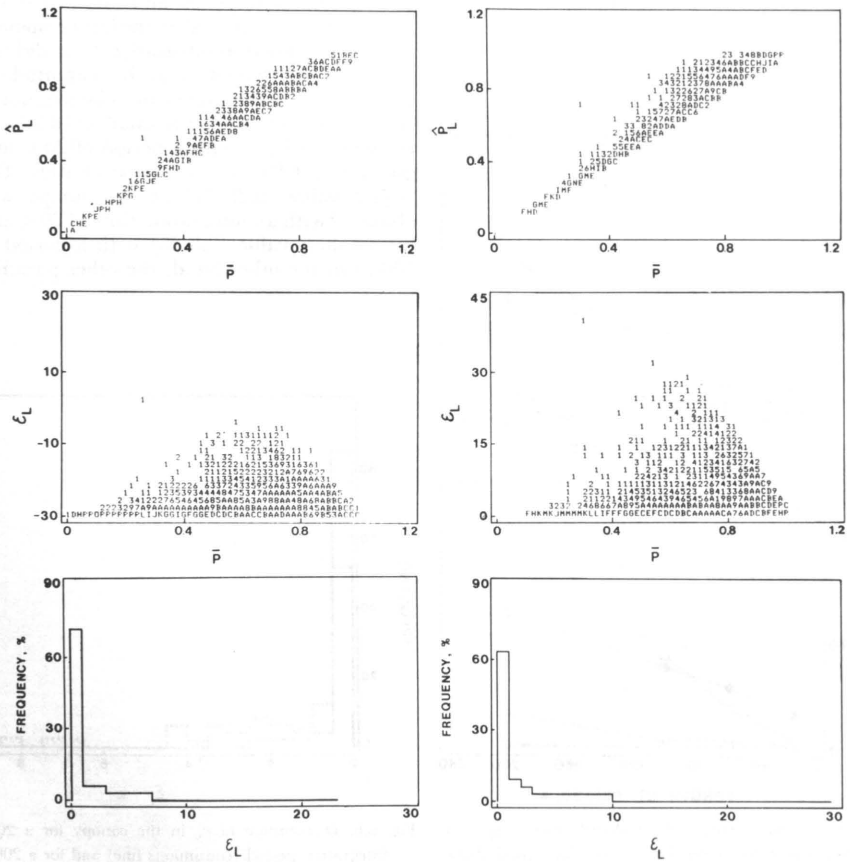

Fig. 6.7. $\hat{P}_L$ and ε_L as a function of $\bar{P}$ and frequency distribution of ε_L in data set C (July 10, 19 and 27, cloudy days). Symbols are the same as in Fig. 4.17.

SWECON researchers in the use of linear integration (Linder and Troeng 1980).

The result also shows that shortening the length of the measuring period is an effective way of decreasing the error due to linear approximation caused by variation within the measuring period. Reducing the length of the measuring period in the open from 100 s to 20 s reduces the mean error to one quarter, and within stands to one half. Shortening the integration period within this time range cannot essentially affect the magnitude of the maximum error, but instead makes the occurrence of significant errors unlikely. However, the fact that significant errors still do occur in the material should be taken into account in the analysis of the data. Thus there is reason to use a more robust method, which puts a smaller weight on diverging observations, in the estimation of the environmental responses of photosynthesis, in place of the least square sum method (e.g. Kennedy and Gentle 1980).

The results given by linear integration for data set C (Eos measurements) are presented in Fig. 6.7. Only data for cloudy days (July 10, 19 and 27) have been used in the calculation. The errors in this material are considerably greater: the mean error for the shoot light curve is 1.5 % and for the needle light curve 2.2 %, the maximum values being 24 % and 41 %, respectively. This means that integration of the photosynthetic radiation response over longer periods inside the canopy is liable to result in marked bias.

612. Integration over time and space

In addition to the temporal variation in the light falling on a shoot in the canopy, there is also very strong spatial variation (Section 5). For this reason it is necessary to integrate over both time and space in measurements carried out inside the canopy. It is clear that the introduction of spatial variation will increase the total variation of the measuring period, and hence increase the error due to linear approximation.

The error as a result of the light conditions within the canopy is examined here on the basis of data sets A and B. There were 19 sensors spaced at 1.5 cm intervals (the distance between sensors 15 and 16 was 3.0 cm) in data set A, and 15 sensors at 3 cm intervals in data set B. The former case is equivalent to the length of a normal chamber, and the latter is clearly longer than the measuring cuvettes normally in use.

Observed values of ε_L are presented with respect to $\bar{P}$ for data sets A and B in Fig. 6.8. The cluster of points follows a similar pattern obtained by integrating over time only in the open or in the canopy. However, the errors for over- time and over-space integration are greater; the observed maximum error in the case of the shoot light curve is 8.5 %, and the mean error in data set A 1.6 %. The corresponding values are 8.3 % and 1.5 % for data set B. The error in the case of the shoot light curve is in most cases still acceptable, because in data set A the upper quartile is 2.7 % and in data set B 2.3 % (Fig. 6.9). The distributions of the error are still L-shaped. In the case of the needle light curve, linear integration results in a considerably poorer result. The maximum error in data set A is 13.7 %, and data set B 10.5 %. The means of the error are 2.7 and 1.8 % respectively.

The temporal and spatial microvariation within various integration periods of 100 seconds that result in different errors are illustrated in Fig. 6.10. The error appears to increase in proportion to the variation and to the number of observations located on both sides of the saturation area of the curve.

Linear integration is a proper method in certain cases when making measurements within the canopy, despite the rather large maximum error. This is because the upper quartile values of the error are, in the case of the shoot light curve, of the order of 3 %. This is of the same order of magnitude as the accuracy of the IRGA measurements. The magnitude of the upper quartile of the error for the needle light curve, 6 %, is even smaller than the accuracy of the open IRGA system under ideal conditions. However, the fact that the expected value of ε_L is not zero, must be taken into account when interpreting the results.

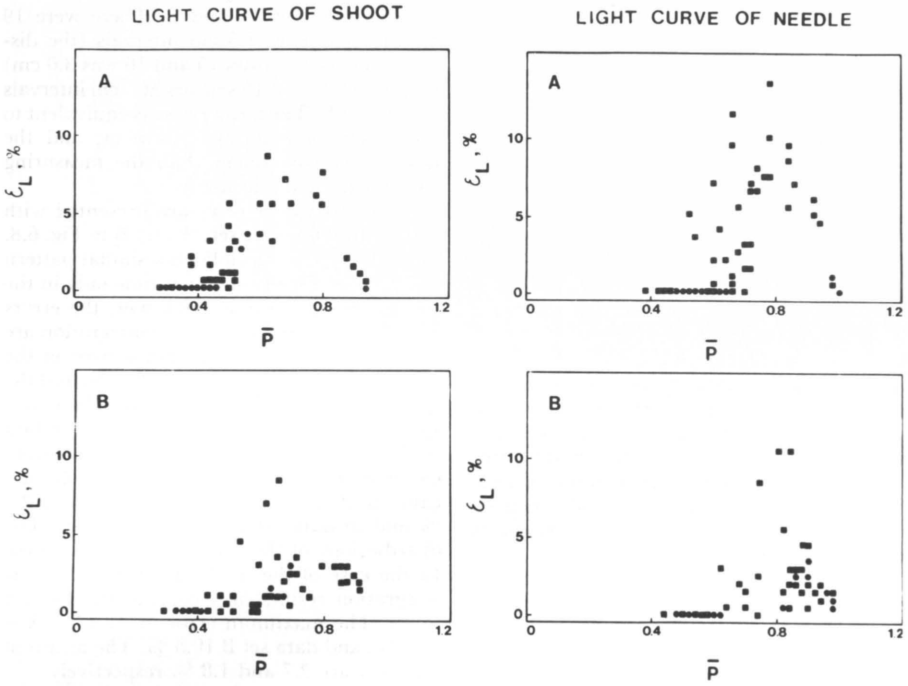

Fig. 6.8. ε_L as a function of $\bar{P}$ in data set A and in data set B. Symbols are the same as in Fig. 6.1.

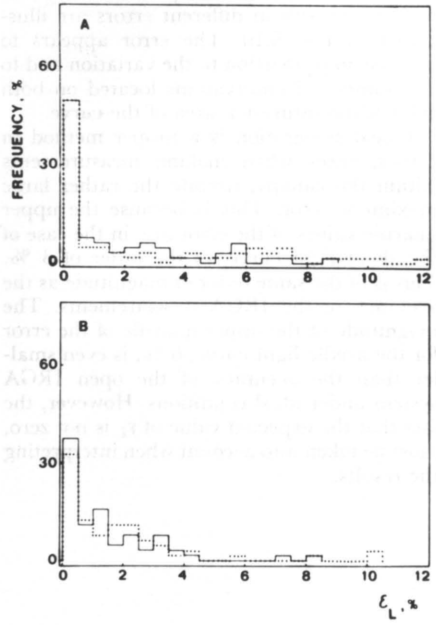

Fig. 6.9. Distributions of ε_L in data set A and B. The solid line represents the shoot light curve and the dotted line the needle light curve.

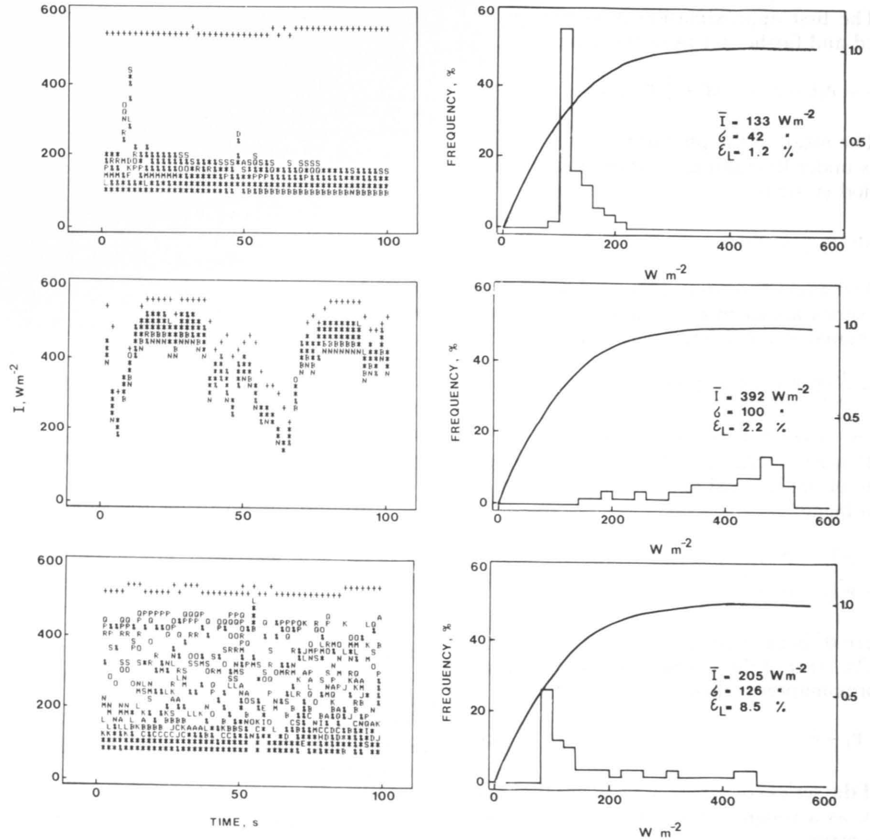

Fig. 6.10. Examples of different integration periods of 100 second in data set A. On the left, the irradiance of 19 sensors (A . . . S) in the canopy and the irradiance above the canopy (+) are plotted as a function of time. On the right, the irradiance distribution of the period is presented with respect to the needle light response curve of photosynthesis.

62. Taylor series approximation

In the previous section the error due to linear approximation under certain conditions was examined empirically. The problem can be approached theoretically using Taylor's series approximation (e.g. Thorneley 1976). The starting point is the same equation (Eq. 2.1) that was used in the numerical analysis of the linear approximation:

$$P = P(I)$$

If the irradiance changes from the initial value I_0 by the amount ΔI, then according to Taylor's formula we get the corresponding "photosynthesis":

$$\begin{aligned} P(I) &= P(I_0+\Delta I) \qquad (6.1) \\ &= P(I_0)+P'(I_0)(\Delta I)+\frac{1}{2!}P''(I_0)(\Delta I)^2+\frac{1}{3!}P'''(I_0)(\Delta I)^3\ldots \\ &= \sum_{m=0}^{\infty}\frac{1}{m!}P^{(m)}(I_0)(\Delta I)^m \end{aligned}$$

The first approximation is to neglect the third and further terms of the series:

$$P(I) = P(I_0)+P'(I_0)(\Delta I)+\frac{1}{2!}P''(I_0)(\Delta I)^2 \qquad (6.2)$$

The mean of the photosynthesis which occurs under fluctuating irradiance in the time period (t_0,t_1) is:

$$\bar{P}(t_0,t_1) = \frac{1}{n}\sum_{i=1}^{n} P(I_i) \qquad (6.3)$$

And again according to second order Taylor series approximation, when the series is evaluated at mean irradiance, $\bar{I}$:

$$\hat{P}_T = \frac{1}{n}\left(\sum_{i=1}^{n} P(\bar{I})+\sum_{i=1}^{n} P'(\bar{I})\Delta I+\frac{1}{2}\sum_{i=1}^{n} P''(\bar{I})(\Delta I)^2\right) \qquad (6.4)$$

The second term in parentheses in Eq. (6.4) is zero because $\sum_{i=1}^{n} \Delta I = 0$, the approximate of the integral of the response function then being:

$$\hat{P}_T = P(\bar{I})+\frac{1}{2}P''(\bar{I})\frac{1}{n}\sum_{i=1}^{n}(\Delta I)^2 \qquad (6.5)$$
$$= P(\bar{I})+\frac{1}{2}P''(\bar{I})\cdot\sigma^2$$

where σ^2 is the variance of I.

The error of the second order Taylor series approximation is then:

$$\varepsilon_T = \hat{P}_T - \bar{P} \qquad (6.6)$$

If the series converges, we can use the third term as a rough estimate of the approximation error.

$$\varepsilon_T \approx \frac{1}{3!}P'''(\bar{I})\frac{1}{n}\sum_{i=1}^{n}(\Delta I)^3 \qquad (6.7)$$

Use of the second order Taylor series expansion means that the function to be integrated is approximated by the parabola (Eq. 6.8) in such a way that approximation at the evaluation point of the series is accurate up to the second derivate:

$$P(Q) = P(\bar{I})+P'(\bar{I})(\Delta I)+\frac{1}{2}P''(\bar{I})(\Delta I)^2 \qquad (6.8)$$

where: $\bar{I}$ is the mean irradiance
Q is the actual irradiance
$\Delta I = Q - \bar{I}$

In this method the wrong function is thus integrated over the correct distribution. This is based on the fact that it is sufficient for integrating the parabola over the distribution G if the first and second centre moment (u_1 and u_2) of the distribution are known:

$$\int(ax^2+bx+c)dG = a\int x^2dG + b\int xdG + c\int dG \qquad (6.9)$$
$$= au_2 + bu_1 + c$$

The use of second order Taylor series approximation is illustrated in Fig. 6.11. The accuracy of the approximation thus depends on the behaviour of the higher derivatives of the light curve used. Linear integration means that the function is approximated using the line which is a tangent to the curve drawn at the point of mean irradiance.

The second order Taylor series gives a rather good approximation which is close to the mean irradiance. For example, when the mean irradiance is 240 Wm^{-2}, approximation is accurate enough in the range of ± 100 Wm^{-2} around the mean for the shoot light curve. In the case of the needle light curve the range is ± 50Wm^{-2}. The second order Taylor series approximation thus appears to be a rather good method in the case of limited variation in irradiance. The more convex the response curve, the more confined is the allowable variation for a satisfactory approximation.

The passage of the derivatives of the light curves is described in Fig. 6.12. The derivatives are presented in the equation form in the Appendix. The second derivative, which describes the concavity of the curve and which is used in the approximation, is always negative. The minimum value ($-0.477\cdot10^{-4}$) of the second derivative of the needle curve occurs at the point 145 Wm^{-2}, and the corresponding value for the shoot curve ($-0.156\cdot10^{-4}$) is at the point 140 Wm^{-2}. The absolute value of the minimum value of the second derivative of the needle curve is about three times the minimum value of the second derivative of the shoot curve. For this reason, the same variance produces a larger error in linear approximation in the case of the needle light curve if the mean irradiance falls on the minima of the second derivative of the curve.

The second order Taylor series approximation gives a rather accurate estimate for $\bar{P}$ in the case of the shoot light curve (Fig. 6.13, data sets A and B together, integrated over time and space). The estimate for $\bar{P}$ hardly improves at all in the case of the needle light

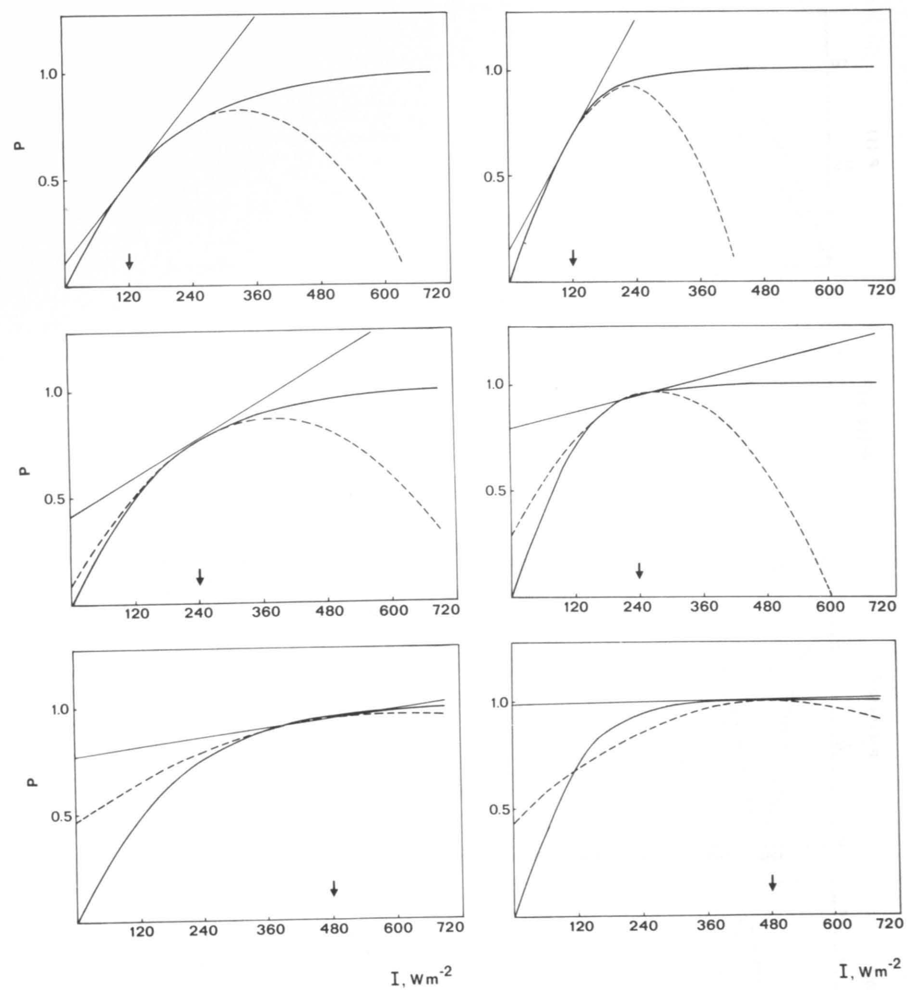

Fig. 6.11. The second order Taylor series expansion (dashed line) approximates the response function (thick line) around the mean irradiance (arrow) over a wider range of irradiance values in the case of the shoot light curve (on the left) than the needle light curve (on the right). Use of linear approximation means that the response function is approximated with the tangent in the mean irradiance (thin line).

curve, but the overestimate given by linear integration alone changes into an underestimate (Fig. 6.14). In addition, an almost unbiased estimate is obtained with the correction term in the case of the shoot light curve, since the mean error is very close to zero (Fig. 6.15A). The results obtained for data set C using second order Taylor series approximation are presented in Fig. 6.16. The variation within the integration period was greater in this data set. The mean error in the case of the shoot light response curve decreases from

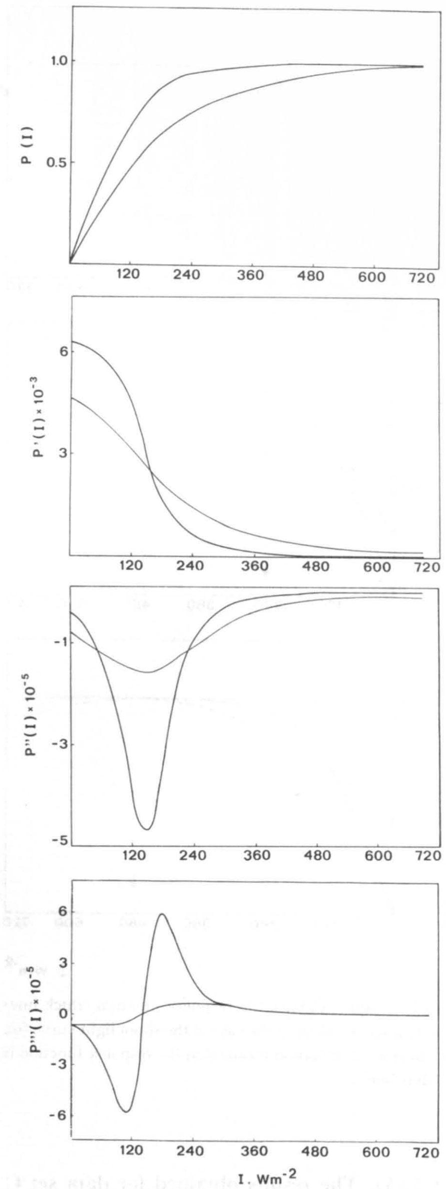

Fig. 6.12. The photosynthetic light response curves used in calculations, and their derivatives. The thick line depicts the shoot light curve and the thin line the needle light curve.

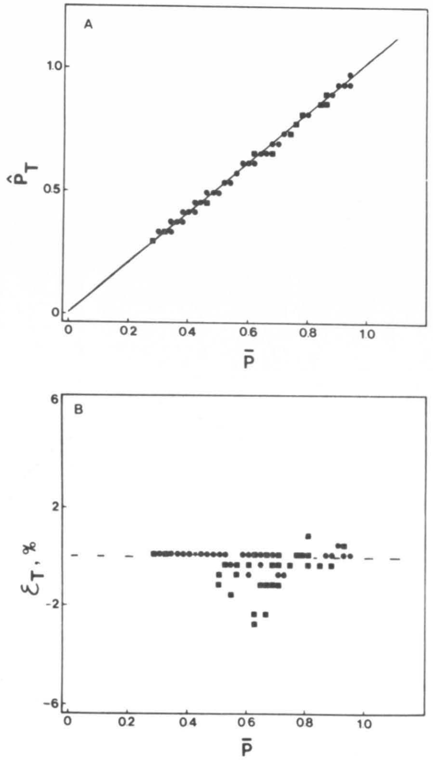

Fig. 6.13. $\hat{P}_T$ and ε_T as a function of $\bar{P}$ in the case of the shoot light curve (data sets A and B). Symbols are the same as in Fig. 6.1.

1.5 to −0.3 %, and the maximum error from 24 % to −16 %. The approximation gave poor results for the needle light curve; the mean error changed from 2.2 % to −1.2 %, and the maximum error increased from 41 % to −73 %. In this respect, the results support the graphic analysis presented earlier.

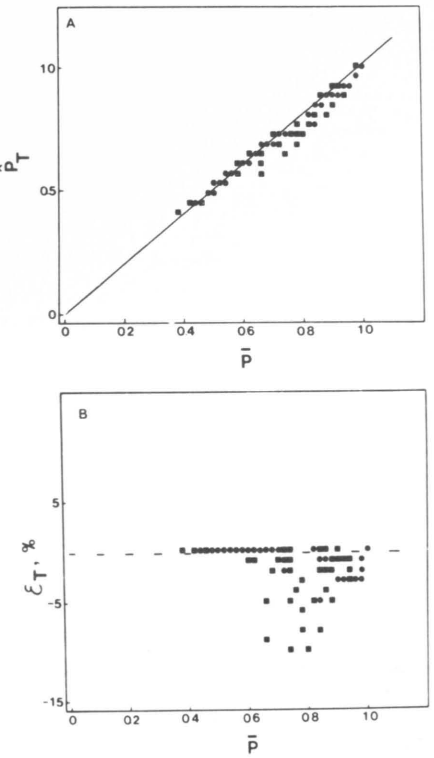

Fig. 6.14. $\hat{P}_T$ and ε_T as a function of $\bar{P}$ in the case of the needle light curve. Symbols are the same as in Fig. 6.1.

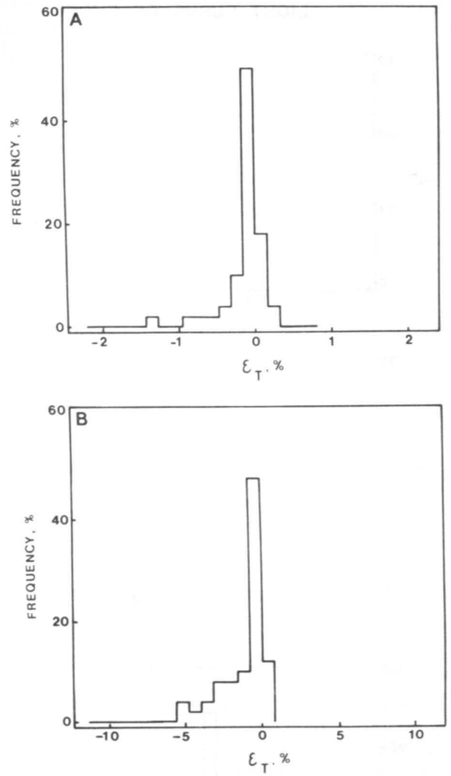

Fig. 6.15. Distributions of ε_T for the shoot light response curve (A) and the needle light response curve (B).

63. Distribution approximation

As the earlier presented method is based on the approximation of the light curve with second order Taylor series integrated over the actual distribution, an opposite procedure is tested in the following; the exact curve is integrated over the approximated distribution. The more moments of the distribution are known in the approximation, either measured or based on an assumption, the more sophisticated is the method which can be applied.

The distributions of irradiance of the integration periods do not have any simple shape on which we could base the approximation. Thus we used the crude two-point distribution (see Rosenblueth 1981), having its non-zero probabilities equal and the standard deviation from the mean;

$$I_1 = \bar{I} - \sigma$$
$$I_2 = I + \sigma \qquad (6.10)$$

This is a special case of the more general antithetic variate techniques (Kleijnen 1974). This distribution has the same mean and the same variance as the true distribution. When the correct response function is 'integrated' over the approximating two-point distribution, we get an estimate, $\hat{P}_D$:

$$\hat{P}_D = \frac{1}{2}\,(P(I_1) + P(I_2)) \qquad (6.11)$$

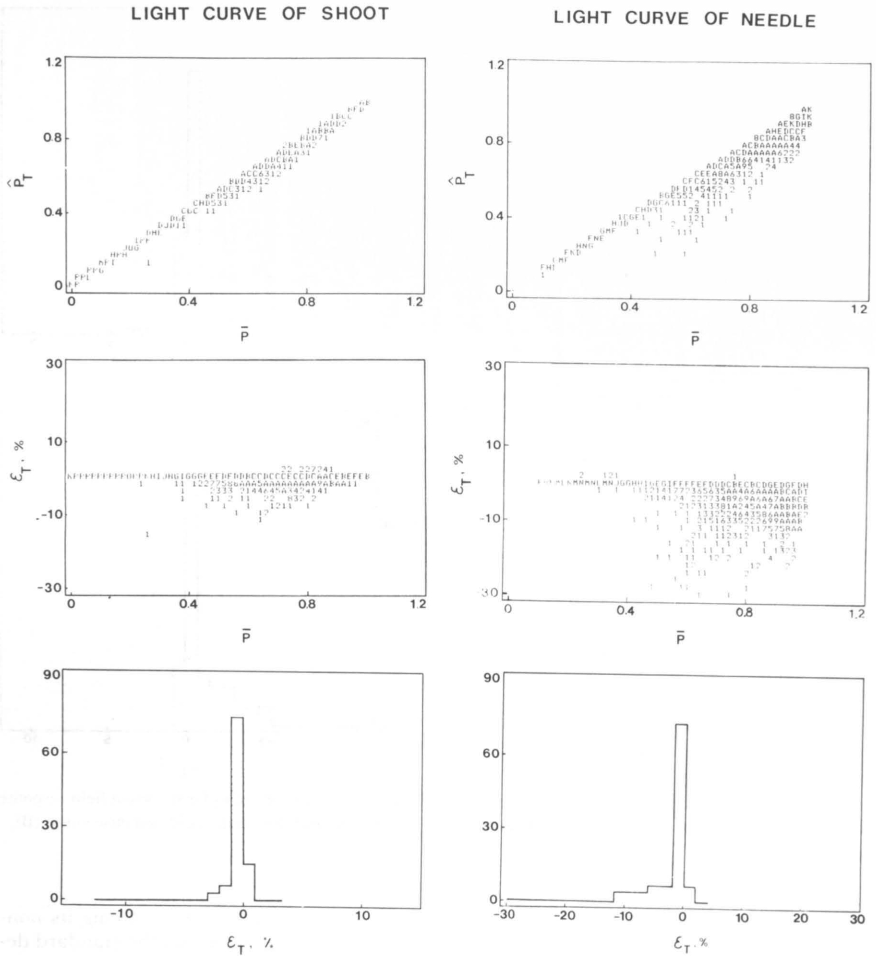

Fig. 6.16. Results of second order Taylor series approximation on data set C (cf. Fig. 6.7).

The principle of the two-point distribution approximation is presented in Fig. 6.17.

In the case of the shoot light curve, the results do not essentially differ from the results given by the second order Taylor series approximation (Fig. 6.18). In the case of the needle light curve, the results are considerably better since the maximum of the error is now only 4 % (Fig 6.19). A special feature is that the method appears to produce an almost unbiased estimate for $\bar{P}$, since the mean error (0.04 %) is very close to zero (Fig 6.20).

The results given by the two-point distribution approximation for data set C are presented in Fig. 6.21. In this material the results are also essentially better in the case of the needle light response curve than the results obtained with second order Taylor series approximation. The mean error in the case of the shoot light curve decreases from 1.5 % to –0.14 % and the maximum error from 41 % to –24 %.

The method based on approximation of the distribution thus appears to give as good results as the second order Taylor series approximation in the case of the low-curvature response, and clearly better in the case of the high-curvature response. It can be shown theoretically that if the Taylor series approximation gives a good estimate for $\bar{P}$, then the distribution method will do that too. However, the distribution method can also give a good approximation in cases where second order Taylor series approximation gives a poor estimate of $\bar{P}$. This is due to the fact that when the variance is large and the distribution extreme, approximation of the function with a parabola (cf. Fig. 6.16) can give a very biased result. The distribution method, which involves integration of the "right" function over the wrong distribution, is not as

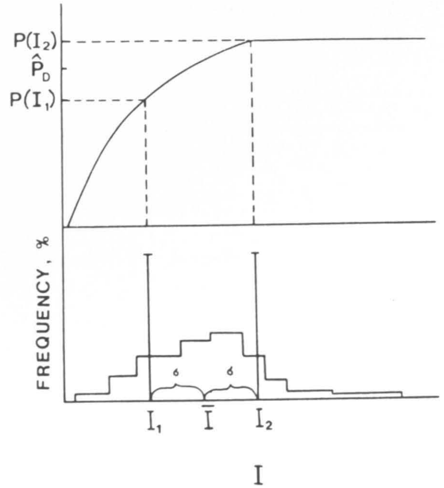

Fig. 6.17. Schematic representation of the two point distribution approximation.

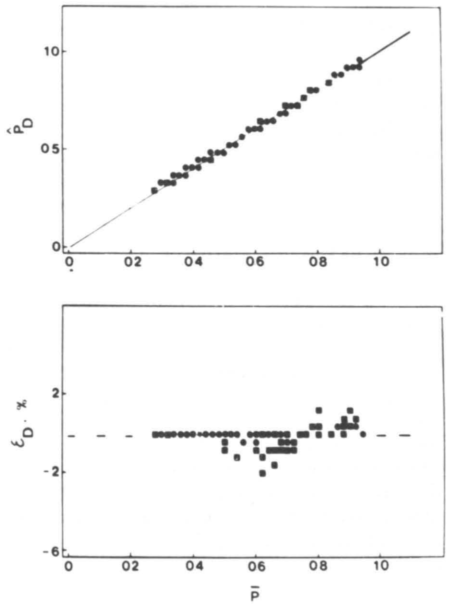

Fig. 6.18. $\hat{P}_D$ and ε_D as a function of $\bar{P}$ in the case of the shoot light curve (data sets A and B). Symbols are the same as in Fig. 6.1.

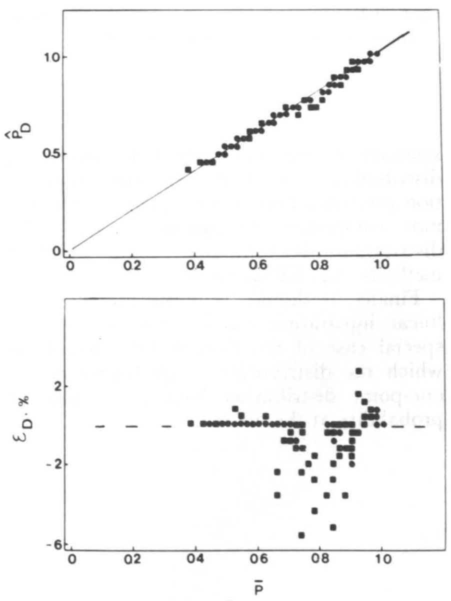

Fig. 6.19. $\hat{P}_D$ and ε_D as a function of $\bar{P}$ in the case of the needle light curve. Symbols are the same as in Fig. 6.1.

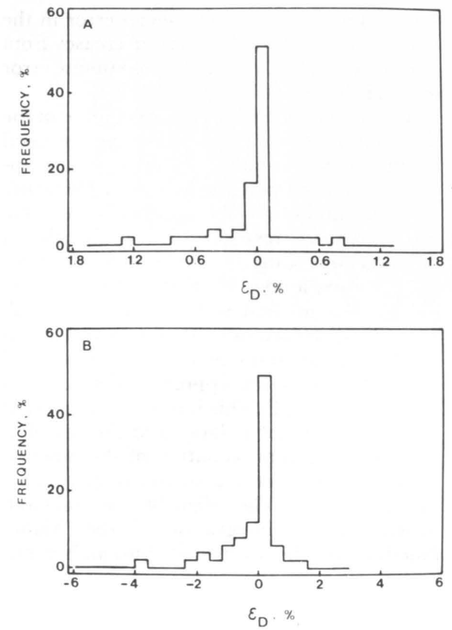

Fig. 6.20. Distributions of ε_D in the case of the shoot light curve (A) and the needle light curve (B).

sensitive to large variation and a diverging distribution. Use of the two-point distribution presented here is a simple example of a more comprehensive approach in which the distribution is estimated using different methods (e.g. Kilkki 1979).

Finally, it should be borne in mind that linear integration can be interpreted as a special case of the distribution method in which the distribution is approximated by one-point distribution having its nonzero probability at the mean.

64. A method for measuring the variation of irradiance

We can conclude that linear integration can be applied to measure microvariation in the irradiance rather well in cases of limited variation. In cases of high variability in irradiance, the variance during the integration period should be known. Thus it is possible to approximate nonlinear integrals using second order Taylor series approximation or two point distribution approximation. However, the second order Taylor series approximation gave poor results for the high-curvature response. The two-point distribution approximation gave good results also in the case of a high-curvature light response. The great advantage of these methods is that it is not necessary to know the light response of photosynthesis in the measurement phase. A fixed light response curve is a disadvantage of nonlinear integration.

The variance can be measured on the basis of integration of the second power of the irradiance, since the variance can be expressed as:

$$\sigma^2 = \frac{\Sigma I^2 - (\Sigma I)^2/N}{N} \qquad (6.12)$$

Nowadays, integration of the square is easily realized with digital techniques. It is thus possible to achieve the advantages of nonlinear integration by summing the irradiance and its square, without being restricted to a known light response curve. The advantage of this measuring principle would, in addition, be its physical clarity because the photosynthetically usable light is obtained numerically on the basis of the mean density of the radiation flux and its variance.

The unbiasness of the methods can be increased by measuring, in addition to the mean and the variance, also higher order moments of the distribution. Every new moment means a new variable to be stored, and the higher the moment in question, the less the amount of new information it provides. In most cases the method based on the measurement of the mean and the variance is sufficient.

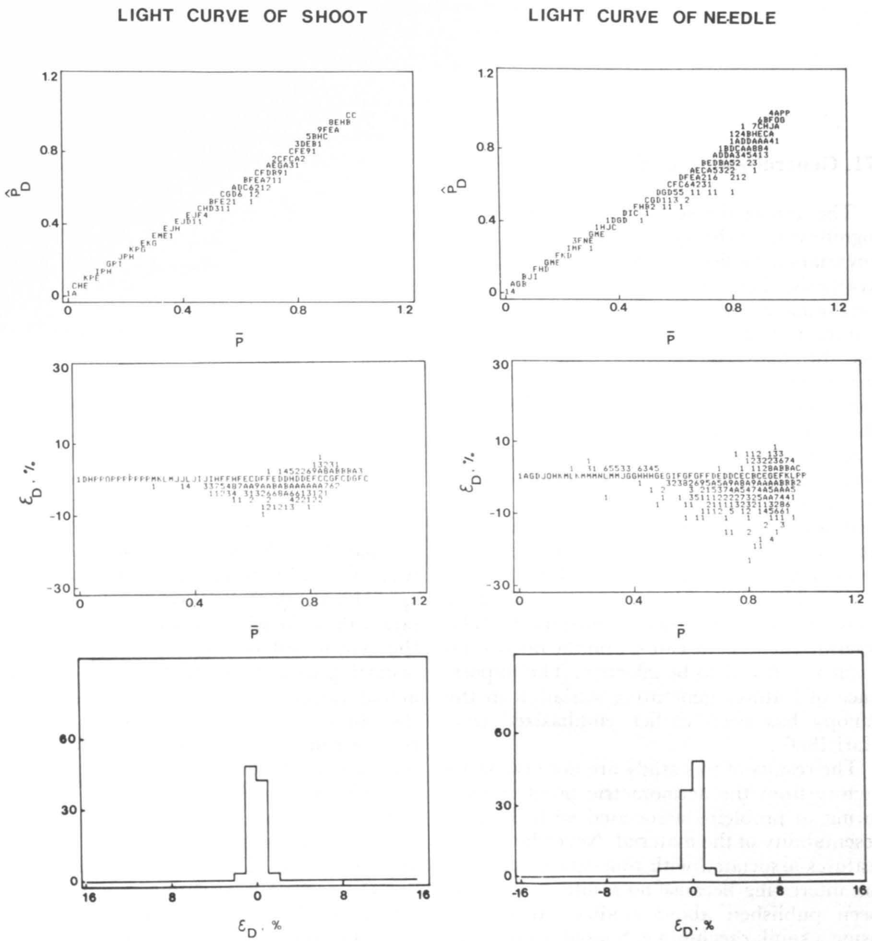

Fig. 6.21. Results of two-point distribution approximation on data-set C (cf. Fig. 6.7).

7. DISCUSSION

71. Generalization of the results

The aim of the study was to evaluate the significance of the spatial and temporal microvariation in field measurements of photosynthesis. The study can be regarded as a preliminary examination of the time-space variation in the canopy of a Scots pine stand. As the material comprises measurements made at one site over a shorter period of time, the results of the autocorrelation analyses and the variation analyses should be regarded with caution. The results are only indicative, and values of the parameters vary depending on the weather type, and at different points within the stand. The results of the variation analyses were evaluated using a more representative material (data set C) and the results showed that the estimates of variation were of the same order of magnitude. The filtering effect of the canopy on the microvariation was found to be effective. The importance of features generating variation in the canopy has been earlier emphasized (e.g. Hari 1980).

The results of this study are not very satisfactory from the actinometric point of view owing to problems associated with the representability of the material. Nevertheless the features associated with time-space variation are interesting because no results have so far been published about studies carried out using a similar technique. Spatial microvariation is usually measured using the scanning technique in which the measurements made at different places are also made at different times (e.g. Norman and Tanner 1969, Niilisk et al. 1970). A method in which the time-space variation is stored as such for processing, could provide a very effective tool for studying the temporal and spatial variation in the light in the crown canopy as a stochastic process. The sampling problems in a pine stand which is horizontally very heterogenous are, however, very great in comparison to those in more homogenous stands such as cereals and willows.

A theoretical preliminary analysis of the sources of variation has apparently led to an approach of a different kind. For instance, Oker-Blom and Kellomäki (1983) have theoretically shown that the proportion of shading within the crown is considerably larger than the shading between crowns in a pine stand. In this respect the location of the sensor array used here was ineffective. An analysis restricted to one shoot within the crown would have made interpretation of the results easier.

In addition, the properties of the sensors have to be considered when interpreting the results. Although the measuring head of the sensor was rather small (diameter 6 mm) compared to the sensors generally used, it was still too big from the point of view of the spatial variation, because its diameter was larger than the width of a single needle. Thus the sensor did not record all the variation occurring with respect to space and time. The actual variation was apparently larger than the observed because in some cases part of the measuring head was in the full shade, part half-shade, and part in full light illuminated by a sun fleck.

The restrictions described above also apply to the analyses of the error due to linear approximation. The presented error values due to linear approximations are thus underestimates. The bias due to linear approximations for the 10-minute periods measured using the Eos-system was considerably larger, but the mean error for even a period as long as 10 minutes was of the order of 2 %. The restrictions concerning the sensors naturally also apply to the Eos system, which, moreover, includes the loss of information caused by grouping. Although the restrictions of the material do not essentially affect the conclusions made for different integration methods, there is reason to test the results using a more extensive material.

72. Measurement of the light environment of the shoot

Photosynthesis is usually compared to the instantaneous quantum flux density falling on the plane either at the beginning (Koch 1957) or at the end of the measuring period (e.g. Korpilahti 1982). The temporal microvariation has been taken into account in a number of studies by comparing photosynthesis to the mean irradiance during the measuring period (e.g. Linder et al. 1980). However, McCree and Loomis (1969) have stressed that if the measurement of the mean is to be parallelled to photosynthesis, then the output of the sensor should be nonlinear with respect to irradiance in the same way as photosynthesis is. Hari et al. (1976) developed equipment based on nonlinear integration for field studies of photosynthesis. Kellomäki et al. (1979) used equipment working on the same principle for estimating photosynthesis on the basis of the photosynthetically available irradiance.

The problems associated with the measurement of the radiation environment have been considered rather little in field measurements of photosynthesis, although the difficulties with the measurement of irradiance have been documented in actinometric studies (e.g. Andersson 1964, McCree 1965, Ross 1970). The effect of the structure of the radiation climate has also been described under laboratory conditions. When measuring the photosynthesis of coniferous shoots in a diffuse radiation field, Zelawski et al. (1973) found that the structure of both the light climate and the needle distribution on the shoot have a large effect on shoot photosynthesis. The fact that these results have not influenced the methods used in field measurements of photosynthesis is at least partly due to the common use of black-box models. Black-box models are very effective when the aim is to obtain preliminary information about the factors affecting a process, but their use is associated with serious problems in ecophysiological studies. For instance, if the structure of a process is not known, then it is difficult to know how the inputs should be described so that the description would be valid with respect to the output.

The problems associated with validity become especially large when studying physiological adaptation mechanisms. When studying the acclimation of photosynthesis under shading by measuring shoot light response curves, the differences in the shape of the response curve can be interpreted to be due to physiological changes in the needles. However, considerable differences may be due to the structure of the needle foliage on the shoot, e.g. needle angle differs on light and shade shoots (Leverenz 1980b). Interpretation of the light response curves of photosynthesis calculated from field data is also associated with similar problems, because the direction distribution of the radiation does not remain the same throughout the growing season.

In this study, variation analysis and numerical simulations of different integration methods were used in evaluating the importance of microvariation in radiation for photosynthesis studies. It was concluded that taking the microvariation into account presupposes integration. Nonlinear integration involves methodological problems in the analysis of the data, with the result that a certain light response curve has to be relied on. Therefore, the possibilities of avoiding these problems were studied here.

Of the three methods examined in this study – linear integration, nonlinear integration involving approximation of the response function using second order Taylor series, and the approximation of distribution – the distribution approximation method proved to be the most promising. The second order Taylor series approximation gave good results in the case of a low-curvature light response, but did not essentially improve the results with a high-curvature light response in comparison to linear integration. Linear integration also gave rather accurate results especially with short integration times, but the unsatisfactory feature of this method is the bias of the results.

Both Taylor series approximation and the distribution approximation were examined in cases where the second moment of the distribution is known. Both methods are thus clarified cases of the correction methods commonly used in the removal of bias caused by non-linearity (e.g. Kilkki 1979). The form of the irradiance distribution thus cannot be taken as known as it varies from case to case considerably. The existence of upper and lower limits introduces some regularity to the form of the distribution in cases of high variance, as described in Section 42. The skewed two-point distribution based on correlation between the mean irradiance and skewness of the distribution gives probably less bias than the symmetric distribution. The main aim of further studies should be to find methods which give distribution approximations that are sufficiently reliable and which apply efficient measurement procedures.

Lappi and Smolander (1984) described a method for calculating the exact bounds of mean photosynthesis for any mean and variance combination of irradiance. This theoretical analysis showed that for many mean and variance combinations second order Taylor series approximation does not give feasible estimates, i.e. there does not exist an irradiance distribution with the given mean and variance that would lead to the estimated mean photosynthesis. On the contrary, two-point distribution gives feasible estimates for all mean variance combinations.

A number of recent studies have criticised the comparison of photosynthetic rate to the radiation flux density falling on a plane (Leverenz and Jarvis 1979, Leverenz 1980b, Oker-Blom et al. 1983). These studies have shown that the structure of needle foliage on the shoot, as well as the position of the shoot with respect to the direction of the radiation beams, produces considerable differences in the light response of shoot photosynthesis. Oker-Blom et al. (1983), for instance, observed a 100 % increase in photosynthetic rate in the nonsaturated area when the angle between the branch and the light beam was changed from 0° to 90°. The light response of the shoot is thus the sum of the light responses of the individual needles. Owing to the differing position of the needles with respect to the direction of the incoming radiation, as well as mutual shading by the needles, the light response of the shoot can differ considerably from the light response of the needles (e.g. Leverenz 1980b). The light response of an individual needle is thus more invariant from the point of view of physiology than that of the shoot. However, it is a challenging measuring problem because it presupposes a new type of micromeasurement system for gas exhange. For the time being we have to measure gas exhange on the shoot level.

How then should the light environment of the shoot be described during photosynthesis measurements? The following discussion, based on the results of this study and other studies concerned with measurement geometry, is more the presentation of a research task than the description of a developed method.

There are two components in the light environment of the shoot. First, the incoming radiation flux varies with respect to time and space. Second, the relationship between the geometry of the needle foliage on the shoot and the directional distribution of the radiance determines the irradiance distribution on the surface of the needles. Oker-Blom et al. (1983) have presented a model in which this irradiance distribution can be calculated in the direct radiation field from a number of properties of the needle foliage. However, neither diffuse radiation nor the penumbra-effect have yet been taken into account in this model. In recent work these features were incorporated in the model (Oker-Blom 1984). The description of the light environment of the shoot in field measurements of photosynhesis could be carried out as outlined in Fig. 7.1.

It is assumed that the variation in the diffuse radiation is so small with respect to space and temporally so slow that it can be regarded in the model as a uniform "background radiation" during the measurement period. Thus the mean and the variance of the global radiation could be obtained using the integral of the first and second power. The distribution of radiation flux could be further estimated from this information using distribution approximation. The model would calculate, the irradiance distribution on the surface of based on three sources of data (see Fig. 7.1): 1) on the basis of the data concerning the radiation flux, 2) the geometry of the shoot and 3) direction of incoming radiation. The direction distribution of the radiation can be calculated on the basis of the date, time of day and amount of diffuse radiation.

Finally, the light responses, e.g. for different temperature classes, could be estimated from the irradiance distributions on the needle surface and from the corresponding photosynthetic rate. Estimation of the light response of photosynthesis is slightly more complicated by the method described than by the methods which have been used up to now. Because one photosynthetic rate observation does not have a single value to describe the light environment, it should be characterized using the irradiance distribution on the surface of the needles.

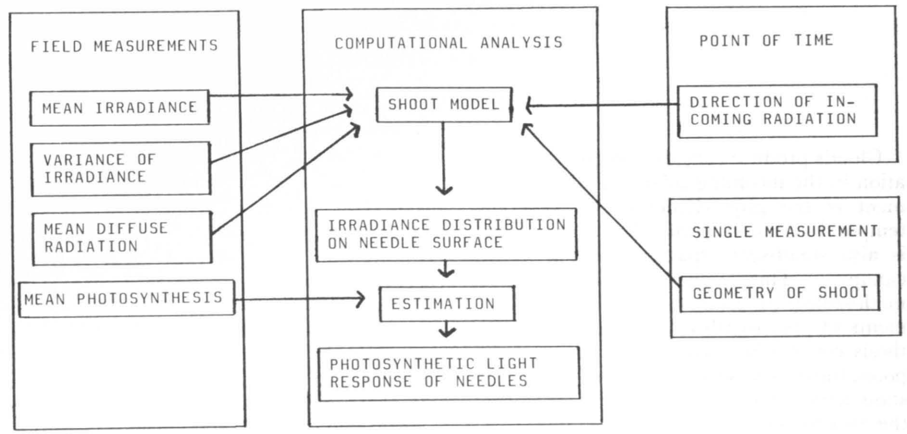

Fig. 7.1. Schematic outline for describing the light environment of a shoot in field studies of photosynthesis.

If approximation of nonlinear integration based on second order Taylor series approximation is used, then the correct parameters have to be found by iterative means. This is because the values of the parameters have to be assumed for derivatives. In this respect the distribution method is more simple.

In studies where the light response curve of the needle photosynthesis is assumed to be known, the above method can be used to estimate the shoot photosynthesis from radiation observations if the geometrical properties of the shoot are known. This type of study could be applied to examine the significance of the structure of the needle foliage for the photosynthesis in different light environments.

Radiation energy and the saturation deficit of the air are the driving forces for transpiration. Therefore, the presented method would obviously be suitable for transpiration studies, because the irradiance distribution at the surface of the needles gives an estimate of the radiation energy falling directly on the needle foliage. The method could be applicable for monitoring the connections between photosynthesis and transpiration. If it is assumed that the environmental response of transpiration is known, then the transpiration of the shoot can be estimated in the same way as for photosynthesis. In principle, it would be possible to study, using the simulation technique, the effect of the structure of the needle foliage on the efficiency of water consumption in different environments.

Measurements in accordance with physical principles, i.e. linear integration, supplemented with description of the variation, thus appear to offer many advantages as a basis for describing the light environment of the shoot. As it was earlier shown, the method of nonlinear-approximation gives as almost a good result as nonlinear integration but concurrently avoids the disadvantages of nonlinear integration. In addition, the method provides an opportunity to consider the effects of the geometrical properties of the shoot. The last but not the least important feature is that the method is also applicable for characterizing the radiation environment of the shoot in terms of transpiration.

8. SUMMARY

Clouds produce considerable periodic variation in the incoming solar radiation. Movement of the phytoelements also generates temporal variation within the canopy. There is also small-scale spatial variation in the canopy. This microvariation causes methodological problems in field measurements of photosynthesis. Because photosynthesis can not be measured at such a small point, the irradiance could be considered constant with respect to time and place during the measurement.

The temporal and spatial microvariation is first described using variation and autocorrelation analysis on an empirical material. The importance of the microvariation for photosynthesis studies is determined by examining the integration problem caused by the variation.

The results of variation analysis showed that the problems caused by temporal microvariation can be effectively reduced by shortening the measurement period. Reducing the length of the measuring period over the range 20–200 s does not essentially decrease the maximum values of the within-period variation, but it does significantly decrease the relative proportion of the periods with large variability. Invariance was not found in the stochastic properties of the variation with autocorrelation analysis as the autocorrelation functions varied widely.

The spatial variation was considerable during sunny periods since the mean of the within 30 cm distance standard deviation was 66 Wm^{-2} when the irradiance varied in the range 60–560 Wm^{-2}. The spatial microvariation was very small during overcast periods.

The microvariation of the irradiance should be taken into account in the measurements by integrating the irradiance in the open over time and also over space within the canopy. The non-linearity of the light response of photosynthesis produces bias in the results if linear integration is used. According to the results, the error produced by temporal microvariation is of the order of 0.5 % during a period of 100 s, the maximum error being under 10 %. When the spatial and the temporal microvariation are considered, the mean error for a 100-second period is 1 % and the maximum error about 10 %. The error for the high-curvature light response (needle light curve) was greater than that for the low-curvature light response (shoot light curve). Since the error increases as variation increases, the error can be effectively decreased by reducing the time-space dimension of the measurements.

Approximation of nonlinear integration using second order Taylor series approximation proved to be rather accurate in the case of the low-curvature light response, since the mean error decreased from 1.6 %to 0.2 %. The second order Taylor series approximation gave poor results for the high-curvature light response.

The two-point distribution approximation gave accurate estimates for the low and high-curvature light curve: the mean error decreased from 2.7 % to 0.4 % and maximum error from 14 % to 4.5 %. The distribution method was not as sensitive to the extreme distributions and convexity of the response curve as second order Taylor series approximation.

The results are used to demonstrate a new light measuring method for field measurements of photosynthesis and also for actinometric measurements within stands. When the first power (mean) and the second power (variance) of irradiance are integrated, the nonlinear integrals can be estimated accurately enough and the estimates are almost unbiased afterwards.

The main advantage of the proposed method is that it is not necessary to resort to a certain light curve during the actual measurements and the disadvantages of nonlinear integration are thus avoided. Furthermore, the geometry of the shoot can be taken into account. The method is also applicable to transpiration studies since transpiration increases linearly, as opposed to photosynthesis, with respect to the irradiance.

REFERENCES

Acock, B., Thornley, J. H. M. & Warren Wilson, J. 1970. Spatial variation of light in the canopy. In: Prediction and measurement of photosynthetic productivity. (Ed. Šetlik, J.). Pudoc, Wageningen: 91–102.

Anderson, M. C. 1964. Light relations of terrestrial plant communities and their measurement. Biol. Rev. 39: 425–486.

— 1966. Some problems of simple characterization of the light climate in plant communities. In: Brainbridge et al (Eds) Light as an ecological factor. Blackwell, Oxford: 77–90.

— 1970. Radiation climate, crop architecture and photosynthesis. In: Prediction and measurement of photosynthetic productivity (ed. Šetlik, J.). Pudoc, Wageningen: 71–78.

— 1971. Radiation and crop structure. In: Plant photosynthetic production. Manual of methods (ED. Šestak, Z., Čatský & Jarvis, P. G.) Dr W. Junk N. V. Publishers, The Hague: 412–456.

Bartlett, M. S. 1966. Stochastic processes. Cambridge, Univ. Press. 362 p.

Blackman, R. B. & Tukey, J. W. 1958. The measurement of power spectra. Dover Publications, New York. 190 p.

Charles-Edwards, D. A. 1981. The mathematics of photosynthesis and productivity. Academic Press. 127 p.

— & Ludwig, L. J. 1974. A model for leaf photosynthesis by C_3-plant species. Ann. Bot. 38: 921–930.

Chartier, P. 1970. A model of CO_2 assimilation in the leaf. In: Prediction and measurement of photosynthetic productivity (Ed. Šetlik, J.). Pudoc, Wageningen: 307–315.

Christersson, L. & Sandstedt, R. 1968. Short-term temperature variation in needles of *Pinus silvestris* L. Can. J. For. Res. 8: 480–482.

Farquhar, G. D., von Caemmerer, S. & Berry, J. A. 1980a. A biochemical model of photosynthetic CO_2 assimilation in leaves of C_3 species. Planta 149: 78–90.

— Schulze, E.-D. & Kuppers, M. 1980b. Responses to humidity by stomata of *Nicotiana glauca* L. and *Corylus avellana* L. are consistent with the optimatization of carbon dioxide uptake with respect to water loss. Aust. J. Plant. Physiol. 7: 315–327.

— & Sharkey, T, D. 1982. Stomatal conductance and photosynthesis. Ann. Rev. Plant. Physiol. 33: 317–345.

Gaastra, P. 1959. Photosynthesis of crop plants as influenced by light, carbon dioxide, temperature, and stomatal diffusion resistance. Meded. Landbouwhogesch. Wageningen 59(13): 1–68.

Gates, D. M. 1980. Biophysical ecology. Springer-Verlag New York–Heidelberg–Berlin. 611 p.

Hallman, E., Hari, P., Räsänen, P. & Smolander, H. 1978. The effect of planting shock on the transpiration, photosynthesis, and height increment of Scots pine seedlings. Seloste: Istutusshokin vaikutus männyntaimien transpiraatioon, fotosynteesiin ja pituuskasvuun. Acta For. Fenn. 161: 1–26.

Hari, P. 1980. The dynamics of metabolism in a plant community. Flora 170: 28–50.

– Hallman, E., Salminen, R. & Vapaavuori, E. 1981. Evaluation of factors controlling net photosynthetic rate in Scots pine seedlings under field conditions without water stress. Oecologia 48: 186–189.

– Kanninen, M., Kellomäki, S., Luukkanen, O., Pelkonen, P., Salminen, R. & Smolander, H. 1979. An automatic system for measurements of gas exhange and environmental factors in a forest stand, with special reference to measuring principles. Seloste: Metsikön kaasuaineenvaihdon ja ympäristötekijöiden automaattinen mittausjärjestelmä. Silva Fennica 13(1): 94–100.

— , Kellomäki, S., Mäkelä, A., Ilonen, P., Kanninen, M., Korpilahti, E. & Nygren, M. 1982. Metsikön varhaiskehityksen dynamiikka. Summary: Dynamics of early development of tree stand. Acta For. Fenn. 177: 1–42.

— , Nilson, T., Salminen, R., Kaipiainen, L., Korpilahti, E. & Ross, J. 1984. Nonlinear dependence of photosynthetic rate on irradiance and its consenquenses for estimates of the amount of saccharides formed. Photosynthetica 18(1): 28–33.

— , Salminen, R., Pelkonen, P., Huhtamaa, M. & Pohjonen, V. 1976. A new approach for measuring light inside the canopy in photosynthesis studies. Seloste: Uusi maastokelpoinen valon mittausmenetelmä yhteyttämistutkimuksia varten. Silva Fennica 10(2): 94–102.

— , Sievänen, R. & Salminen, R. 1983. On measuring in plant ecological studies. Flora 173: 63–70.

Jarvis, P. G., Eckard, F. E., Koch, W. & Čatský, J. 1971. Examples of assimilation chambers in current use. In: Prediction and measurement of photosynthetic productivity (Ed. Šetlik, J.). Pudoc, Wageningen: 84–104.

Kaufmann, M. R. 1981. Automatic determination of conductance, transpiration, and environmental conditions in forest trees. Forest Sci. 27(4): 817–827.

Kellomäki, S. & Oker-Blom, P. 1983. Canopy structure and light climate in a young Scots pine stand. Seloste: Männikön latvuston rakenne ja latvuston sisäiset valaistusolot. Silva Fenn. 17(1): 1–21.

— , Salminen, R., Hari, P., Ventilä, M., Kanninen, M., Kauppi, P. & Smolander, H. 1979. A method for approximating the photosynthetic production of stand members inside the canopy. J. Appl. Ecol. 16: 243–252.

Kennedy, W. Jr. & Gentle, J. E. 1980. Statistical computing. Marcel Decker, New York. 591 p.

Kilkki, P. 1979. Outline for a data processing system in forest mensuration. Silva Fenn. 13(4): 368–384.

Kleijnen, J. P. C. 1974. Statistical techniques in simulation. Marcel Dekker, Inc. New York, 775 p.

Koch, W. 1957. Der Tagesgang der "productivität der Transpiration". Planta 48: 418–452.

Korpilahti, E. 1982. Istutusta edeltäneen kuivatuksen vaikutus männyn taimien fotosynteesiin ja kasvuun. Metsänhoitotieteen laitoksen tiedonantoja 37: 1–96.

Lange, O. L. 1962. Eine Klapp-Kuvette zur CO_2-Gaswechselregistrierung an Blättern von Freilandspflanzen mit dem URAS. Ber. Dtsch. Bot. Ges. 75: 41–50.

Lappi, J. & Smolander, H. 1981. Reaaliaikainen tiedonkeruu toteutettuna yliopiston metsäaseman PDP 11/34-pientietokoneella. Summary: Real time data time data collecting with a PDP 11/34 computer at the University of Helsinki Forestry Field Station. Helsingin yliopiston metsänhoitotieteen laitoksen tiedonantoja 31: 1–17.

— & Smolander, H. 1984. Integration of the hyperbolic radiation-response function of photosynthesis. Photosynthetica 18(3): 402–410.

Leverenz, J. 1980 a. Convexity and net quantum efficiency of the light response curve of photosynthesis. In: Understanding and predicting tree growth (Ed. S. Linder). Swed. Conif. For. Proj. Techn. rep. 25: 120–124.

— 1980 b. Shoot structure and productivity in conifers. In: Understanding and predicting tree growth (ed S. Linder). Swed. Conif. For. Proj. Techn. Rep. 25: 135–137.

— & Jarvis, P. G. 1979. Photosynthesis in Sitka spruce (*Pices sitchensis* (Bong.) Carr.) VIII. The effect of light flux density and direction on the rate of net photosynthesis and the stomatal conductance of needles. J. Appl. Ecol. 16: 919–932.

— & Jarvis, P. G. 1980. Photosynthesis in Sitka spruce (Picea *sitchensis* (Bong.) Carr.) IX. The relative distribution made by needles to photosynthesis by the shoot. J. Appl. Ecol. 17:59–68.

Linder, Sp., Nordstöm, B., Parsby, J., Sundbom, J. & Troeng, E. 1980. A gas exhange system for field measurements of photosynthesis and transpiration in a 20-year-old stand of Scots pine. Swed. Conif. For. Proj. Tech. Rep. 23: 1–34.

— & Troeng, E. 1980. Photosynthesis and transpiration of 20-year-old Scots pine. In: Structure and function of northern coniferous forests – An ecosystem study (Ed. Persson, T.). Ecol. Bull. (Stockholm) 32: 165–181.

Marshall, B. & Biscoe, P. V. 1980 a. A model for C_3 leaves describing the dependence of net photosynthesis on irradiance. I. Derivation. J. Exp. Bot. 31(120): 29–39.

— & Biscoe, P. W. 1980 b. A model for C_3 leaves describing the dependence of net photosynthesis on irradiance. II. Application to the analysis of flag leaf photosynthesis. J. Exp. Bot. 31(120): 41–48.

McCree, K. J. 1965. Light measurements in plant growth investigations. Nature 206: 527.

— & Loomis, R. S. 1969. Photosynthesis in fluctuating light. Ecology 50(3): 422–428.

Mustachi, C., Cena, V. & Rocchi, M. 1979. Stochastic simulation of hourly global radiation sequences. Solar Energy 23: 47–51.

Niilisk, H., Nilson, T. & Ross, J. 1970. Radiation in plant canopies and its measurement. In: Prediction and measurement of photosynthetic productivity. (Ed. Šetlik, J.). Pudoc, Wageningen. 165–177.

Nilson, T. 1971. A theoretical analysis of the frequency of gaps in plant stands. Agric. Meteorol. 8: 25–38.

Norman, J. M. & Tanner, C. B. 1969. Transient light measurement in plant canopies. Agron. J. 61: 847–849.

Oker-Blom, P. 1984. Photosynthesis of a Scots pine shoot: Simulation of irradiance distribution and distribution of a shoot in different radiation fields. Agric. Meteorol. (in print).

— & Kellomäki, S. 1983. Effect of grouping of foliage on the within-stand and within-crown light regime: Comparison of random and grouping canopy models. Agric. Meteorol. 28: 143–155.

— , Kellomäki, S & Smolander, H. 1983. Photosynthesis of Scots pine shoot: The effect of shoot inclination on the photosynthetic response of a shoot subjected to direct radiation. Agric. Meteorol. 29: 191–206.

Pelkonen, P. 1980. The uptake of carbon dioxide in Scots pine during spring. Flora 169: 386–397.

— 1981. Investigations on seasonal CO_2-uptake in Scots pine. II. The autumn fall in CO_2-uptake in Scots pine. Seloste: Tutkimuksia männyn hiilidioksidin kulutuksen vuodenaikaisvaihtelusta. II. Hiilidioksidin kulutuksen heikkeneminen syksyllä. Commun. Inst. For. Fenn. 99 (5): 21–39.

Raschke, K. 1956. Mikrometeorologish gemessene Energie umsatze eines Alocasiablattes. Archiv. fur Meteorologie, Geophysik und Bioklimatologie, Ser B 7 (2): 240–268.

Rosenblueth, E. 1981. Two-point estimates in probabilities. Appl. Math. Modelling 5: 229–335.

Ross, J. 1970. Mathematical models of photosynthesis in a plant stand. In: Prediction and measurement of photosynthetic productivity (Ed. Šetlik, J.). Pudoc, Wageningen. 29–43.

— 1981. The radiation regime and architecture of plant stands. Dr. W. Junk Publishers, The Hague-Boston-London. 399 p.

Salminen, R., Hari, R., Kellomäki, S., Korpilahti, E., Kotiranta, M. & Sievänen, R. 1983. A measuring system for estimating frequency distribution of irradiance within plant canopies. J. Appl. Ecol. 20: 887–895.

— & Ventilä, M. 1979. Metsäekologinen tiedonkeruujärjestelmä. Sähkö 52 (7–8): 206–209.

Schulze, E.-D., Hall, A. E., Lange, O. L. & Walz, H. 1982. A portable steady-state porometer for measuring the carbon dioxide and water vapour exhanges of leaves under natural conditions. Oecologia 53: 141–145.

Snedecor, G., W. & Cochran, W., G. 1980. Statistical methods. (7th ed.). The Iowa State University Press. 507p.

Szeicz, G. 1974. Solar radiation for plant growth. J. Appl. Ecol. 11: 617–636.

Thornley, J. H. M. 1976. Mathematical models in plant physiology. Academic Press, London. 318 p.

Troeng, E. & Linder, S. 1978. Gasutbytet hos ett 20-årigt tallbeståndt. IV. Ettåriga barrs fotosyntes och transpiration i olika delar av trädkronan. Abstract: Gas exchange in a 20-year-old stand of Scots pine. IV. Photosynthesis and transpiration within the crown of one tree. Swed. Conif. For. Proj. Int. Rep. 83: 1–23.

Zelawski, W., Szaniawski, R., Dybczynski, W. & Piechurowski, A. 1973. Photosynthetic capasity of conifers in diffuse light of high illuminance. Photosynthetica 7: 351–357.

Total of 68 references

SELOSTE

SÄTEILYN VAIHTELUN MITTAAMINEN FOTOSYNTEESIN MAASTOTUTKIMUKSISSA

Pilvet aiheuttavat tulosäteilyyn ajoittain voimakasta vaihtelua. Latvustossa oksien liikkeet lisäävät ajallista vaihtelua. Latvustossa esiintyy myös pienimuotoista paikan suhteen tapahtuvaa vaihtelua. Molemmat mikrovaihtelut aiheuttavat fotosynteesin maastotutkimuksissa metodisia ongelmia, sillä fotosynteesiä ei pystytä mittaamaan niin pistemäisesti, että valon intensiteettiä voitaisiin pitää vakiona ajan ja paikan suhteen.

Työssä on aluksi kuvattu empiiristen aineistojen perusteella valon intensiteetin ajallista ja paikallista mikrovaihtelua hajonta- ja autokorrelaatiotarkastelujen avulla. Tämän jälkeen on tutkittu vaihtelun merkitystä fotosynteesitutkimusten kannalta tarkastelemalla vaihtelun aiheuttamaa integrointiongelmaa.

Hajontatarkastelut osoittivat, että ajallisen mikrovaihtelun aiheuttamia ongelmia voidaan vähentää tehokkaasti lyhentämällä mittausjaksoa. Mittausjakson lyhentäminen alueella 20–200 s ei tosin olennaisesti pienennä jakson sisäisen hajonnan maksimiarvoja, mutta se pienentää voimakasta vaihtelua sisältävien jaksojen suhteellista osuutta. Autokorrelaatiotarkastelujen avulla ei löydetty invarianssia vaihtelun luonteesta, vaan autokorrelaatiofunktiot olivat hyvin erityyppisiä eripituisina jaksoina.

Paikan suhteen tapahtuva vaihtelu oli aurinkoisina jaksoina huomattavaa, sillä 30 cm:n matkalla esiintynyt hajonta oli keskimäärin 66 W/m^2, kun säteily vaihteli alueella 60–560 Wm^{-2}. Paksun pilvipeitteen aikana paikallinen vaihtelu oli hyvin pientä.

Työssä tullaan johtopäätökseen, että säteilyn mikrovaihtelu on otettava huomioon mittaustilanteessa integroimalla irradianssi aukealla ajan ja latvustossa lisäksi paikan yli. Fotosynteesin valovasteen epälineaarisuus aiheuttaa harhaa tuloksiin, mikäli käytetään lineaarista integrointia (keskiarvoa). Tulosten mukaan ajallisen mikrovaihtelun aiheuttama harha 100 sekunnin jaksoilla on puolen prosentin luokkaa maksimivirheiden ollessa alle 10 %:n. Kun ajallisen mikrovaihtelun lisäksi otetaan huomioon myös paikallinen mikrovaihtelu, kuten latvuston sisällä tehtävissä mittauksissa joudutaan tekemään, on harha 100 sekunnin jaksolle prosentin ja maksimivirhe kymmenen prosentin luokkaa. Harha on jyrkälle valokäyrälle (neulasten valovaste) suurempi kuin loivalle (verson valovaste). Koska virhe kasvaa hajonnan kasvaessa, niin virhettä voi pienentää tehokkaasti lyhentämällä mittauksen aika-paikka-ulottuvuutta.

Epälineaarisen integroinnin approksimointi Taylorin sarjan avulla, kun sarjakehitelmä katkaistiin toiseen termiin, osoittautui loivan valokäyrän (verson valokäyrä) tapauksessa varsin toimivaksi, sillä harha pieneni 1,6 %:sta 0,2 %:iin. Sarjakehitelmä antoi jyrkälle valokäyrälle (neulasen valokäyrä) huonoja tuloksia, sillä harha kasvoi n. 1,6 kertaiseksi lineaarisen integroinnin käyttöön verrattuna.

Jakauma-approksimaatioon perustuva menetelmä antoi hyviä tuloksia paitsi loivalle myös jyrkälle valokäyrälle: Harha pieneni 2,7 %:sta 0,4 %:iin ja maksimivirhe 14 %:sta 4,5 %:iin. Jakaumamenetelmä ei siten ollut yhtä herkkä käyrän jyrkkyydelle ja poikkeaville jakaumille kuin Taylorin sarjakehitelmä.

Tulosten perusteella työssä esitetään uusi valonmittausmenetelmä fotosynteesin maastomittauksia ja kasvustojen aktinometrisia mittauksia varten. Kun mittausvaiheessa integroidaan säteily (keskiarvo) lisäksi sen neliö (varianssi) niin epälineaarinen integrointi voidaan tehdä useimmiten riittävän harhattomasti vasta laskentavaiheessa.

Ehdotetun menetelmän keskeinen etu on, ettei mittaustilanteessa tarvitse sitoutua tiettyyn fotosynteesin valovasteeseen, mikä on epälineaarisen integroinnin harmillinen piirre. Toiseksi menetelmää käytettäessä on mahdollista ottaa huomioon mittauskohteen, esim. verson geometria. Menetelmä on lisäksi sovelias haihduntatutkimuksiin, sillä haihdunta kasvaa, toisin kuin fotosynteesi, lineaarisesti säteilyn suhteen.

Appendix. Nonrectangular hyperbola and its 1st, 2nd and 3rd derivative.

$$P(I) = \frac{1}{2\theta}\left[\alpha I + P_{max} - \left((\alpha I)^2 + P_{max}^2 - \alpha I P_{max}(4\theta - 2)\right)^{\frac{1}{2}}\right]$$

$$P'(I) = \frac{1}{2\theta}\left[\alpha - \left[(\alpha I)^2 + P_{max}^2 - \alpha I P_{max}(4\theta - 2)\right]^{-\frac{1}{2}} \cdot \left[\alpha^2 I - \alpha P_{max}(2\theta - 1)\right]\right]$$

$$P''(I) = \frac{1}{2\theta}\left[\left[(\alpha I)^2 + P_{max}^2 - \alpha I P_{max}(4\theta - 2)\right]^{-\frac{3}{2}} \cdot \left[\alpha^2 I - \alpha P_{max}(2\theta - 1)\right]^2 - \alpha^2\left[(\alpha I)^2 + P_{max}^2 - \alpha I P_{max}(4\theta - 2)\right]^{-\frac{1}{2}}\right]$$

$$P'''(I) = \frac{1}{2\theta}\left[-3\left((\alpha I)^2 + P_{max}^2 + \alpha I P_{max}(2 - 4\theta)\right)^{-\frac{5}{2}} \cdot \left(\alpha^2 I - \alpha P_{max}(2\theta - 1)\right)^3 + 3\alpha^2\left((\alpha I)^2 + P_{max} + \alpha I P_{max}(2 - 4\theta)\right)^{-\frac{3}{2}} \left(\alpha^2 I - \alpha P_{max}(2\theta - 1)\right)\right]$$

ODC 111.21--015+111.84 ISBN 951-651-064-7

SMOLANDER, H. 1984. Measurement of fluctuating irradiance in field studies of photosynthesis. Seloste: Säteilyn vaihtelun mittaaminen fotosynteesin maastotutkimuksissa. Acta For. Fenn. 187: 1–56.

The problems caused by the temporal and spatial fluctuation of irradiance during field measurements of photosynthesis are studied using irradiance data measured in a Scots pine (*Pinus sylvestris* L.) stand. It is concluded on the basis of variation analysis that the microvariation should be measured by integration. However, the curvilinearity of the light response of photosynthesis results in biased estimates when linear integration (mean irradiance) is used. The errors due to the linear integration were computed. Furthermore, second order Taylor series approximation and two-point distribution approximation in the estimation of mean photosynthesis were studied. Both methods presuppose that the mean and variance (integrals of first and second power) are known. The results indicate, that problems caused by irradiance fluctuation could be avoided by measuring the second power of irradiance.

Author's address: The Finnish Forest Research Institute, Suonenjoki Research Station, SF-77600 Suonenjoki, Finland.

ODC 111.21--015+111.84 ISBN 951-651-064-7

SMOLANDER, H. 1984. Measurement of fluctuating irradiance in field studies of photosynthesis. Seloste: Säteilyn vaihtelun mittaaminen fotosynteesin maastotutkimuksissa. Acta For. Fenn. 187: 1–56.

The problems caused by the temporal and spatial fluctuation of irradiance during field measurements of photosynthesis are studied using irradiance data measured in a Scots pine (*Pinus sylvestris* L.) stand. It is concluded on the basis of variation analysis that the microvariation should be measured by integration. However, the curvilinearity of the light response of photosynthesis results in biased estimates when linear integration (mean irradiance) is used. The errors due to the linear integration were computed. Furthermore, second order Taylor series approximation and two-point distribution approximation in the estimation of mean photosynthesis were studied. Both methods presuppose that the mean and variance (integrals of first and second power) are known. The results indicate, that problems caused by irradiance fluctuation could be avoided by measuring the second power of irradiance.

Author's address: The Finnish Forest Research Institute, Suonenjoki Research Station, SF-77600 Suonenjoki, Finland.

ODC 111.21--015+111.84 ISBN 951-651-064-7

SMOLANDER, H. 1984. Measurement of fluctuating irradiance in field studies of photosynthesis. Seloste: Säteilyn vaihtelun mittaaminen fotosynteesin maastotutkimuksissa. Acta For. Fenn. 187: 1–56.

The problems caused by the temporal and spatial fluctuation of irradiance during field measurements of photosynthesis are studied using irradiance data measured in a Scots pine (*Pinus sylvestris* L.) stand. It is concluded on the basis of variation analysis that the microvariation should be measured by integration. However, the curvilinearity of the light response of photosynthesis results in biased estimates when linear integration (mean irradiance) is used. The errors due to the linear integration were computed. Furthermore, second order Taylor series approximation and two-point distribution approximation in the estimation of mean photosynthesis were studied. Both methods presuppose that the mean and variance (integrals of first and second power) are known. The results indicate, that problems caused by irradiance fluctuation could be avoided by measuring the second power of irradiance.

Author's address: The Finnish Forest Research Institute, Suonenjoki Research Station, SF-77600 Suonenjoki, Finland.

ODC 111.21--015+111.84 ISBN 951-651-064-7

SMOLANDER, H. 1984. Measurement of fluctuating irradiance in field studies of photosynthesis. Seloste: Säteilyn vaihtelun mittaaminen fotosynteesin maastotutkimuksissa. Acta For. Fenn. 187: 1–56.

The problems caused by the temporal and spatial fluctuation of irradiance during field measurements of photosynthesis are studied using irradiance data measured in a Scots pine (*Pinus sylvestris* L.) stand. It is concluded on the basis of variation analysis that the microvariation should be measured by integration. However, the curvilinearity of the light response of photosynthesis results in biased estimates when linear integration (mean irradiance) is used. The errors due to the linear integration were computed. Furthermore, second order Taylor series approximation and two-point distribution approximation in the estimation of mean photosynthesis were studied. Both methods presuppose that the mean and variance (integrals of first and second power) are known. The results indicate, that problems caused by irradiance fluctuation could be avoided by measuring the second power of irradiance.

Author's address: The Finnish Forest Research Institute, Suonenjoki Research Station, SF-77600 Suonenjoki, Finland.

ACTA FORESTALIA FENNICA

168 Wuolijoki, E. 1981. Effects of simulated tractor vibration on the psychophysiological and mechanical functions of the driver: Comparison of some exitatory frequencies. Seloste: Traktorin simuloidun tärinän vaikutukset kuljettajan psykofysiologisiin ja mekaanisiin toimintoihin: Eräiden herätetaajuuksien vertailu.

169 Chung, M.-S. 1981. Flowering characteristics of *Pinus sylvestris* L. with special emphasis on the reproductive adaptation to local temperature factor. Seloste: Männyn (*Pinus sylvestris* L.) kukkimisominaisuuksista, erityisesti kukkimisen sopeutumisesta paikalliseen lämpöilmastoon.

170 Savolainen, R. & Kellomäki, S. 1981. Metsän maisemallinen arvostus. Summary: Scenic value of forest landscape.

171 Thammincha, S. 1981. Climatic variation in radial growth of Scots pine and Norway spruce and its importance to growth estimation. Seloste: Männyn ja kuusen sädekasvun ilmastollinen vaihtelu ja sen merkitys kasvun arvioinnissa.

172 Westman, C. J. 1981. Fertility of surface peat in relation to the site type class and potential stand growth. Seloste: Pintaturpeen viljavuuden tunnukset suhteessa kasvupaikkatyyppiin ja puuston kasvupotentiaaliin.

173 Chung, M.-S. 1981. Biochemical methods for determining population structure in *Pinus sylvestris* L. Seloste: Männyn (*Pinus sylvestris* L.) populaatiorakenteesta biokemiallisten tutkimusten valossa.

174 Kilkki, P. & Varmola, M. 1981. Taper curve models for Scots pine and their applications. Seloste: Männyn runkokäyrämalleja ja niiden sovellutuksia.

175 Leikola, M. 1981. Suomen metsätieteellisen julkaisutoiminnan rakenne ja määrällinen kehitys vv. 1909–1978. Summary: Structure and development of publishing activity in Finnish forest sciences in 1909–1978.

176 Saarilahti, M. 1982. Tutkimuksia radioaaltomenetelmien soveltuvuudesta turvemaiden kulkukelpoisuuden arvioimiseen. Summary: Studies on the possibilities of using radar techniques in detecting the trafficability of peatlands.

177 Hari, P., Kellomäki, S., Mäkelä, A., Ilonen, P., Kanninen, M., Korpilahti, E. & Nygrén, M. 1982. Metsikön varhaiskehityksen dynamiikkaa. Summary: Dynamics of early development of tree stand.

178 Turakka, A., Luukkanen, O. & Bhumibhamon, S. 1982. Notes on *Pinus kesiya* and *P. merkusii* and their natural regeneration in watershed areas of northern Thailand. Seloste: Havaintoja männyistä (*Pinus kesiya* ja *P. merkusii*) ja mäntyjen luontaisesta uudistumisesta Pohjois-Thaimaan vedenjakaja-alueilla.

179 Nyyssönen, A. & Ojansuu, R. 1982. Metsikön puutavaralajirakenteen, arvon ja arvokasvun arviointi. Summary: Assessment of timber assortments, value and value increment of tree stands.

180 Simula, M. 1983. Productivity differentials in the Finnish forest industry. Seloste: Tuottavuuden vaihtelu Suomen metsäteollisuudessa.

181 Pohtila, E. & Pohjola, T. 1983. Lehvästöruiskutuksen ajoitus kasvukauden aikana. Summary: The timing of foliage spraying during the growing season.

182 Kilkki, P. 1983. Sample trees in timber volume estimation. Seloste: Koepuut puuston tilavuuden estimoinnissa.

183 Mikkonen, E. 1983. Eräiden matemaattisen ohjelmoinnin menetelmien käyttö puunkorjuun ja kuljetuksen sekä tehdaskäsittelyn menetelmävalinnan apuvälineenä. Abstract: The usefulness of some techniques of the mathematical programming as a tool for the choice of timber harvesting system.

184 Westman, C. J. 1983. Taimitarhamaiden fysikaalisia ja kemiallisia ominaisuuksia sekä niiden suhde orgaanisen aineen määrään. Summary: Physical and physico-chemical properties of forest tree nursery soils and their relation to the amount of organic matter.

185 Kauppi, P. 1984. Stress, strain, and injury: Scots pine transplants from lifting to acclimation on the planting site. Tiivistelmä: Metsänviljelytaimien vaurioituminen noston ja istutuksen välillä.

186 Henttonen, H. 1984. The dependence of annual ring indices on some climatic factors. Seloste: Vuosilustoindeksien riippuvuus ilmastotekijöistä.

187 Smolander, H. 1984. Measurement of fluctuating irradiance in field studies of photosynthesis. Seloste: Säteilyn vaihtelun mittaaminen fotosynteesin maastotutkimuksissa.

188 Pulkki, R. 1984. A spatial database – heuristic programming system for aiding decision-making in long-distance transport of wood. Seloste: Sijaintitietokanta – heuristinen ohjelmointijärjestelmä puutavaran kaukokuljetuksen päätöksenteossa.

189 Heliövaara, K. & Väisänen, R. 1984. Effects of modern forestry on northwestern European forest invertebrates: A synthesis. Seloste: Nykyaikaisen metsänkäsittelyn vaikutukset luoteiseurooppalaisen metsän selkärangattomiin: Synteesi.

190 Suomen Metsätieteellinen Seura 75 vuotta. The Society of Forestry in Finland – 75 years. 1984.

KANNATTAJAJÄSENET – SUPPORTING MEMBERS

CENTRALSKOGSNÄMNDEN SKOGSKULTUR
SUOMEN METSÄTEOLLISUUDEN KESKUSLIITTO
OSUUSKUNTA METSÄLIITTO
KESKUSOSUUSLIIKE HANKKIJA
SUNILA OSAKEYHTIÖ
OY WILH. SCHAUMAN AB
OY KAUKAS AB
KEMIRA OY
G. A. SERLACHIUS OY
KYMI-STRÖMBERG OY
KESKUSMETSÄLAUTAKUNTA TAPIO
KOIVUKESKUS
A. AHLSTRÖM OSAKEYHTIÖ
TEOLLISUUDEN PUUYHDISTYS
OY TAMPELLA AB
JOUTSENO-PULP OSAKEYHTIÖ
KAJAANI OY
KEMI OY
MAATALOUSTUOTTAJAIN KESKUSLIITTO
VAKUUTUSOSAKEYHTIÖ POHJOLA
VEITSILUOTO OSAKEYHTIÖ
OSUUSPANKKIEN KESKUSPANKKI OY
SUOMEN SAHANOMISTAJAYHDISTYS
OY HACKMAN AB
YHTYNEET PAPERITEHTAAT OSAKEYHTIÖ
RAUMA REPOLA OY
OY NOKIA AB, PUUNJALOSTUS
JAAKKO PÖYRY CONSULTING OY
KANSALLIS-OSAKE-PANKKI
SOTKA OY
THOMESTO OY
SAASTAMOINEN YHTYMÄ OY
OY KESKUSLABORATORIO
METSÄNJALOSTUSSÄÄTIÖ
SUOMEN METSÄNHOITAJALIITTO
SUOMEN 4H-LIITTO
SUOMEN PUULEVYTEOLLISUUSLIITTO R.Y.
OULU OY
OY W. ROSENLEW AB
METSÄMIESTEN SÄÄTIÖ
SÄÄSTÖPANKKIEN KESKUS-OSAKE-PANKKI
ENSO-GUTZEIT OY

ISBN 951-651-064-7

Arvi A. Karisto Oy:n kirjapaino
Hämeenlinna 1984